

2093

TE
5092
.MBA3
no. 70-1

~~MISSOURI STATE HIGHWAY DEPARTMENT~~
~~DEPARTMENT OF TRANSPORTATION~~

~~MISSOURI STATE HIGHWAY DEPARTMENT~~
~~DEPARTMENT OF TRANSPORTATION~~

MISSOURI COOPERATIVE HIGHWAY RESEARCH PROGRAM,
REPORT

70-1

Property of
MoDOT TRANSPORTATION LIBRARY

✓✓
"STATIC AND FATIGUE BEHAVIOR OF
CONTINUOUS-COMPOSITE BEAMS WITH
HIGH-STRENGTH BOLTS AS SHEAR CONNECTORS"

36

MISSOURI STATE HIGHWAY DEPARTMENT
UNIVERSITY OF MISSOURI-COLUMBIA
BUREAU OF PUBLIC ROADS



"STATIC AND FATIGUE BEHAVIOR OF CONTINUOUS-COMPOSITE BEAMS WITH
HIGH-STRENGTH BOLTS AS SHEAR CONNECTORS"

TE
5092
M8A3
00.70-1

U.S. DEPARTMENT OF TRANSPORTATION
FEDERAL HIGHWAY ADMINISTRATION

HS-10-171

Prepared for

MISSOURI STATE HIGHWAY DEPARTMENT

by

LAWRENCE N. DALLAM

and

REFIK GURAN

DEPARTMENT OF CIVIL ENGINEERING
UNIVERSITY OF MISSOURI - COLUMBIA
COLUMBIA, MISSOURI

JUNE, 1970

in cooperation with

U.S. DEPARTMENT OF TRANSPORTATION
FEDERAL HIGHWAY ADMINISTRATION
BUREAU OF PUBLIC ROADS

The opinions, findings, and conclusions
expressed in this publication are not necessarily
those of the Bureau of Public Roads.

PB 193105

ABSTRACT

This report deals with some aspects of fatigue and static behavior of continuous composite beams using $3/4$ inch high-strength bolts as shear connectors. Tested in this phase of the program were; (a) nine pushout specimens subjected to repeated loading with varying load ranges, (b) two full scale continuous composite members, one with and one without shear connectors over their negative moment regions, loaded both dynamically and statically, (c) two companion compression pushout specimens, one loaded dynamically and then subjected to a final static loading, one directly subjected to the destructive static loading, and (d) two companion tension pushout specimens, both loaded statically until failure.

Load-slip and fatigue characteristics of the bolted connection were investigated through the testing of the pushout specimens. Load-deflection, load-slip, cycle-slip curves, strain profiles, slip distribution and load-reaction curves were used in the investigation of the full scale composite members. Predicted behavior was compared with the experimental behavior and the cracking patterns were analyzed in detail. Also the members with and without connectors were compared concerning the negative moment region.

The following conclusions were made from this investigation:

1. The magnitude of the critical or yield load and the ultimate load for pushout specimens subjected to fatigue loading (up to 10 million cycles) was essentially the same as those for pushout specimens subjected to static loading.

2. The magnitude of the ultimate load for pushout specimens with two layers of reinforcement in the slabs (Figure 18) was 50% greater than the average ultimate load for pushout specimens with one layer of reinforcement in the slabs (Figure 17). The critical or yield load was not affected by the presence of the additional slab reinforcement.
3. The member with shear connectors over its negative moment region exhibits practically no slip in this region at its working load (approximately 15%) compared with the member lacking such connectors.
4. The absence of shear connectors in the negative moment region increases the slip and the connector force in the positive moment region.
5. The elimination of the shear connectors over the negative moment regions reduces the working and the first yielding loads of a continuous composite member by 30% and 20%, respectively.
6. Elementary beam theory (assuming complete interaction) can satisfactorily be used to predict the behavior of a continuous composite member up to its yield load provided sufficient connection exists and careful consideration is given to slab cracking in the negative moment region.
7. There are fewer cracks (but of greater width) when connectors are placed in the negative moment region.
8. Fatigue is not a factor in the design of composite members using high-strength bolts as shear connectors.

TABLE OF CONTENTS

CHAPTER	PAGE
I. INTRODUCTION	1
1.1 GENERAL	1
1.1.1 Descriptive	1
1.1.2 Background	1
1.1.3 Previous Studies	2
1.2 SCOPE	5
1.3 NOTATION	7
II. TEST SPECIMENS	9
2.1 DESIGN OF COMPOSITE BEAMS	9
2.1.1 Span	9
2.1.2 Steel Beam	9
2.1.3 Concrete Slab	9
2.1.4 Shear Connectors	10
2.2 FABRICATION	11
2.2.1 Materials	11
2.2.2 Preparation for Casting	11
2.2.3 Casting	12
2.2.4 Curing	12
2.3 LOADING	13
2.3.1 Fatigue Loading	13
2.3.2 Static Loading	13
2.4 INSTRUMENTATION	14
2.4.1 Deflection	14
2.4.2 Slip	14
2.4.3 Steel Strain	14
2.4.4 Load Cell	15
2.5 COMPANION SPECIMENS	17
2.5.1 Compression Pushouts	17
2.5.2 Tension Pushouts	17
2.5.3 Concrete Cylinders	18
2.5.4 Tensile Coupons	18
2.5.5 Reinforcing Bar Sections	19
III. TEST PROCEDURES	20
3.1 COMPOSITE BEAMS	20
3.1.1 Preparation of Composite Beams	20

CHAPTER	PAGE
3.1.2	Preparation of Loading for Fatigue 21
3.1.3	Preparation of Loading for Static 21
3.1.4	Loading Procedure 22
3.2	COMPANION SPECIMENS 23
3.2.1	Companion Pushouts 23
3.2.2	Tension Pushouts 24
3.2.3	Concrete Cylinders 25
3.2.4	Tensile Coupons 25
3.2.5	Reinforcing Bar Sections 26
IV.	RESULTS AND COMPARISONS 27
4.1	PUSHOUT TESTS 27
4.2	COMPANION SPECIMEN RESULTS 29
4.2.1	Compression Pushouts 29
4.2.2	Tension Pushouts 30
4.2.3	Concrete Cylinders 31
4.2.4	Tensile Coupons 31
4.2.5	Tension Bar Sections 31
4.2.6	Reinforcing Bar Specimens 32
4.3	COMPOSITE BEAM RESULTS 32
4.3.1	General Observations 32
4.3.2	Analysis 35
4.3.3	Deflection Results 38
4.3.4	Slip Results 38
4.3.5	Reaction Results 39
4.3.6	Strain Results 39
4.4	COMPARISONS 41
4.4.1	Cracking Patterns 41
4.4.2	Beam and Companion Pushouts 42
4.4.3	NCB6FB1 and NCB6FB2 43
V.	SUMMARY AND CONCLUSIONS 45
5.1	SUMMARY 45
5.2	CONCLUSIONS 45
	FIGURES 48
	TABLES 92
	BIBLIOGRAPHY 100

LIST OF FIGURES

FIGURE		PAGE
1	Dimensions and Instrumentation of NCB6FB1	49
2	Dimensions and Instrumentation of NCB6FB2	50
3	Dynamic Loading Apparatus	51
4	Static Loading Apparatus	51
5	Static Load Point	52
6	Placement of Bolts	52
7	Wired Forms	53
8	Supported Forms	53
9	Reinforcing Cage	54
10	Casting	54
11	MTS Control Panel	55
12	MTS Ram	55
13	Instrumentation	56
14	Strain Gage Calibration	56
15a	Load Cell Core	57
15b	Load Cell as Support	57
15c	Load Cell Ready to Use	57
16	Load Cell Wiring	58
17	Fatigue Pushout Specimen	59
18	Beam-Companion Compression Pushout Specimen	60
19	Beam-Companion Tension Pushout Specimen	61
20	Reinforcing - Companion Compression Pushouts	62
21	Reinforcing - Companion Tension Pushouts	62
22	Fatigue Tests on Pushouts	63
23	Tension Test on Pushouts	63
24	Load-Slip Comparison: Non-Companion and Companion	64
25	Non-Companion Pushout Failures	65
26	Companion Compression Pushout Failures	66
27	Load-Slip Comparison: Fatigue and Non-Fatigue	67
28a	Tension Failure - Cracking at Connector	68
28b	Tension Failure - Splitting Slab	68
29	Load-Slip Tension Pushouts	69
30	Typical Tension Failures	70
31	Load-Deflection - Deflection at Load Points	71
32	Slip Distribution at Working Load of NCB6FB1	72
33	Slip Distribution at Working Load of NCB6FB2	73
34	Slip Distribution at Yielding Load of NCB6FB1	74
35	Slip Distribution at Yielding Load of NCB6FB2	75
36	Slip Distribution at Final Load	76
37	Applied Load vs Center Reaction	77
38	Working Strain Profile at Section A	78
39	Yield Strain Profile at Section A	79
40	Working Strain Profile at Section B	80
41	Yield Strain Profile at Section B	81

FIGURE	PAGE
42	Working Strain Profile at Section C 82
43	Yield Strain Profile at Section C 83
44	Negative Flexural Cracking Pattern - NCB6FB1 84
45	Negative Flexural Cracking Pattern - NCB6FB2 84
46	Comparative Cracking Patterns 85
47	Longitudinal Cracking Pattern - NCB6FB1 86
48	Longitudinal Cracking Pattern - NCB6FB2 86
49	Positive Flexural Cracking Pattern - NCB6FB1 87
50	Positive Flexural Cracking Pattern - NCB6FB2 87
51	Applied Load vs Negative Moment 88
52	Load-Slip at a Typical Connector 89
53	Yield Lines at Interior Support - NCB6FB1 90
54	Yield Lines at Interior Support - NCB6FB2 90
55	Connectors Intact After Test 91
56	Separation During Testing - NCB6FB1 91

LIST OF TABLES

TABLE		PAGE
I	Actual Beam Dimensions	93
II	Results of Non-Companion Pushouts	94
III	Results of Static Pushout Tests	95
IV	Results of Companion Compression Pushouts	96
V	Results of Companion Tension Pushouts	96
VI	Results of Cylinder Tests	97
VII	Coupon Results Yield Strength	98
VIII	Coupon Results Static Yield Strength	98
IX	Coupon Results Modulus of Elasticity	98
X	Reinforcing Bar Specimen Results	98
XI	Analyses Results for Test Beams	99

CHAPTER I

INTRODUCTION

1.1 GENERAL

1.1.1 Descriptive The use of shear connectors between a reinforced concrete slab and a structural steel section creates what is called a composite section. The shear connectors fix the two independent parts of the composite section for composite behavior and therefore form a more efficient and a stiffer section. This type of section can be designed with a savings of material and is commonly used in the construction of buildings and bridges.

In general the main advantages of a section that behaves as a composite system rather than as two independent parts can be summarized as, 1) smaller and shallower beams may be used, 2) longer spans are possible without deflection limitations, 3) the toughness or the impact capacity is increased, and 4) the overload capacity of the section is greater (1).

The types of connectors utilized in composite construction vary. Studs, channels, or spirals welded to the steel sections are commonly used to minimize slip between the components. The efficiency and the economic advantages of the composite section depend upon the ability of the connectors to resist slip. For this reason the use of a minimum number of connectors to provide a stiff or rigid connection is desirable for the design of composite sections.

1.1.2 Background The 1966-1967 AASHO Interim Specifications (2) provide a method of design using the elastic theory and the fatigue

properties of welded stud or channel shear connectors; however, these types of connectors provide a rather "flexible" connection between the independent parts of the section.

The allowable design load per connector in the 1965 AASHO Specifications (3) was based upon static loading and a factor of safety of 3.0 on the critical capacity of the connector. The current specifications (2) are based upon the fatigue behavior of the connector and the allowable design load for two million cycles is approximately equal to or less than that of the 1965 specifications. The application of this design criteria results in the use of a large number of connectors in order to satisfy the requirements of the elastic theory.

Another type of connector which has been under extensive testing at the University of Missouri is the high-strength bolt. The bolts, with a washer spot welded to the under side of the heads, are seated in holes predrilled in the top flange of the steel section. After the slab is cast and cured the bolts are tightened providing a very rigid friction-type connection. The elastic design method which assumes no slip between the steel and the concrete is satisfied with considerably fewer connectors of this type.

1.1.3 Previous Studies The testing program for high-strength bolts at the University of Missouri is comprised of several phases.

The first phase of this research program was the testing of twelve pushout specimens (4). The object of this series was to determine some characteristics of the bolts as shear connectors and compare them to the more commonly used connectors.

The connectors tested were $\frac{1}{2}$, $\frac{5}{8}$, $\frac{3}{4}$ inch high-strength

bolts. The conclusions drawn from this investigation were:

- " 1. High-strength pretensioned bolts exhibit practically zero slip in the working range of the load.
2. Bolts attain a critical load or useful capacity that is twice that of studs. The ultimate load is also greater for bolts.
3. There is apparently no loss of prestress (bolt pre-tension) with time in high quality concrete.
4. More research is needed regarding the spacing and edge clearance requirements in haunch members due to the splitting observed in the tests of the pre-stressed specimens. "

The second phase of the research program was an investigation of the behavior of full scale beams. Six simply supported composite beams were loaded to produce positive moment in the beams. The conclusions reached upon completion of the investigation were (5):

- " 1. The load-slip characteristics determined from the tests of the full-scale beams using one-half and five-eighths inch bolt shear connectors compare very favorably with the load-slip characteristics of the companion pushout tests.
2. The ultimate strength of three-fourth inch bolt shear connectors is greater than that found from pushout tests.
3. The elementary beam theory, assuming complete interaction (no slip) between slab and stringer, accurately predicted the deflection and stresses of the composite

beams at service load, even though the shear connectors were designed with little or no factor of safety against slip.

4. The modified ultimate strength theory accurately predicted the ultimate strengths of the composite beams when the ultimate capacities of the shear connectors were known.
5. The high-strength bolt with little or no factor of safety against slip provides a very rigid connection between slab and stringers at service loads and also provides a reserve capacity sufficient to develop the ultimate moment capacity of the fully composite section. "

The third phase of the investigation was done on three full scale composite sections and their companion specimens. The composite beams consisted of a simple span and a cantilever and were loaded to cause negative bending or tension in the slab. The objective of this phase was to study the behavior of the bolts in the negative moment portions of continuous composite members. The findings that were reported are (6):

- " 1. Because of the nature of the load-slip per bolt data for the composite members, a conclusion for the validity of using tension pushouts to predict connector behavior in a member cannot be justified.
2. For those members with connectors over their negative moment regions, there was practically no slip at their working loads, and very little slip (less than

0.01 inches) even at their yielding loads.

3. Elementary beam theory (assuming complete interaction) can be used to satisfactorily predict the behavior at the working loads in the negative moment regions of the members with connectors over the negative moment region.
4. Simple ultimate strength theory can be used to satisfactorily predict the ultimate capacity in the negative moment region of members with connectors over the negative moment regions.
5. The ultimate moment capacity of the member without connectors over the negative moment region exceeded the predicted ultimate capacity of the member with connectors over the negative moment region.
6. The elimination of connectors over the negative moment region of the composite member reduced the working and first yielding loads of that member by approximately 15%. "

1.2 SCOPE

In the fourth phase of the research program nine pushout specimens were loaded with varying intensities of repeated loading to cause fatigue. The publications on the fatigue behavior of welded studs had shown that fatigue was definitely a factor in the design of these connectors (2), (7). It was therefore anticipated that fatigue would also be a factor in the design of high-strength bolt shear connectors. The complete test results of the nine fatigue pushout specimens will be given in later sections of this

report, but the main findings in this study showed that:

1. Fatigue is not a real factor in the behavior of pushouts with high-strength bolt shear connectors.
2. In order to be able to predict the behavior of high-strength bolt connectors in full scale composite sections under fatigue loading, it is necessary to conduct further tests.

In order to further study the fatigue characteristics of high-strength bolts as shear connectors, two full scale beams were designed and tested. Both beams were two span continuous composite sections, one with shear connectors over the negative moment region and one without.

The beams were first subjected to fatigue loading (working load applied for two million cycles) and then loaded statically to the capacity of the testing facilities (200 kips per load point). Also tested in this phase were companion compression and tension pushout specimens for the beams.

The major objectives of this study were:

1. To determine the differences in the behavior of members when shear connectors are eliminated over the negative moment regions.
2. To determine if the results obtained from pushout tests can be used to predict the load-slip and cycle-slip relationships of the composite beams when loaded to produce fatigue.
3. To study the static loading behavior of the negative moment region after applying the service load

for two million cycles.

4. To determine if fatigue is an important factor in the design of full scale composite beams with high-strength bolts as shear connectors.
5. To determine a range (difference between minimum and maximum loads) of load that will cause fatigue failure.
6. To determine the effects of longitudinal cracking on the behavior of the high-strength bolts as shear connectors.

1.3 NOTATION

The composite sections tested in this phase of the investigation were given an alpha-numeric designation in keeping with the previous phases.

For the pushout specimens the first letter, N, indicates normal weight concrete. The second character, 6, denotes the diameter of the connector in eighths of an inch. The next letter, F, shows that the specimen was tested with fatigue loading. The following three characters, 4TB, indicate the number and type of the connector; four high-strength tension bolts. The last numerical value denotes the number of the specimen in the series.

For the companion pushout specimens, a lower case letter was added to the end of the alpha-numeric designation to distinguish the different specimens for each beam. For the companion tension pushout specimens the letter, F, for fatigue changes to, T, for tension.

For the beams the first letter, N, again implies normal weight

concrete. The next two characters, CB, denote full scale continuous beam. The following numerical value, 6, is again the diameter of the connector in eighths of an inch. The last letter, B, signifies the type of connector, high-strength bolts. The final numerical character is the number of the specimen in the series.

CHAPTER II

TEST SPECIMENS

2.1 DESIGN OF COMPOSITE BEAMS

2.1.1 Span Both beams were chosen to have an overall length of 36 feet, since they were to be placed in a testing frame 40 feet in length. Each beam consisted of two 18-foot-continuous spans loaded at center points (Figures 1, 2 and 3). The loading geometry for the static loading differed from that of the fatigue loading, in order to induce transverse bending (Figures 4 and 5).

2.1.2 Steel Beam The steel beams used in the composite sections were 21 WF 55, A-36. The beams arrived in 42 foot lengths, but 4 foot sections were cut off to obtain coupons.

The cross sectional properties varied from those listed in the AISC Manual (8). The values used in the calculations are listed in Table I.

To prevent premature web failure, bearing stiffeners were welded to the beam at each support and additional stiffeners were used at the interior support.

2.1.3 Concrete Slab In keeping with the previous phases of the research program the concrete slab used in this phase was 48 inches wide and 6 inches deep. The length of the slab spanned the full length of the steel section.

The longitudinal reinforcement for both composite sections was in accordance with AASHO Specifications for H-20 loading. It consisted of five number 4 bars placed 11 inches center to center as the

top layer and five number 5 bars also placed 11 inches center to center as the bottom layer. The two layers were separated from each other by means of short reinforcing bar sections welded approximately every four feet to form a cage. The distance between the layers was 2.8 inches center to center. The middle bar in the lower layer was placed only over the negative moment region and extended 42 inches past the calculated contraflexure point at both ends. The transverse reinforcement was also in accordance with the above mentioned specifications to simulate an actual bridge slab. The transverse steel consisted of number 5 bars and was placed 6 inches center to center on both layers of longitudinal reinforcement. For the cross sections of the test beams and their dimensions see Figures 1 and 2.

2.1.4 Shear Connectors The shear connectors used for the test specimens were $\frac{3}{4}$ inch high-strength bolts. Standard $1\frac{3}{4}$ inch diameter mild steel washers were spot welded to the underside of the heads of the bolts. The connectors were then seated in predrilled holes with a clearance of $3\frac{1}{2}$ inches between the top of the flange and the bottom of the washer. In this manner the thread of the bolts was inside the top flange and therefore was not exposed to the concrete.

The spacing of the connectors was designed by both the elastic and the ultimate methods. The allowable values used for the test specimens were obtained from an average of previous pushout tests (4), (5), (6). They were 20 kips per bolt for the elastic and 30 kips per bolt for the ultimate approach for both compression and tension zones and did not include a safety factor. The controlling spacing was obtained from the ultimate approach and the required number of bolts were spaced uniformly along the appropriate sections. The beam

NCB6FB1 was designed with no shear connectors over the negative moment region. NCB6FB2 had the necessary number of connectors over this region to resist connector failure before flexural failure (Figures 1 and 2).

2.2 FABRICATION

2.2.1 Materials The rolled steel sections met the requirements of ASTM A36-66.

The concrete was obtained from a local ready mix plant and consisted of normal weight aggregate and type I portland cement. The fine aggregate was Missouri River sand and the course aggregate was crushed limestone with a maximum size of $\frac{3}{4}$ inch. The mixture was air entrained and typical mix proportions were 1:1.85:3.4 by weight, with a water-cement ratio of 5.0 gallons per sack. This mix was similar to the class B-1 mix used by the State Highway Commission of Missouri for Bridge Construction.

For longitudinal and transverse reinforcement, high-strength steel with a yield of 60,000 psi was used. All bars satisfied the requirements of ASTM A32-62T.

The bolts used as shear connectors were A325, high-strength bolts. The washers were standard mild steel flat head washers.

2.2.2 Preparation for Casting The procedure for casting both beams was identical. The beam was placed on three supports and was stabilized. The holes for the bolts were drilled with a magnetic-base drill (although in practice they would be punched in the shop). The strain gages were then attached to the beam at predetermined points. This procedure will be explained in later sections of this chapter. Next, the bolts were seated against wire chairs and were

tightened to have an overall height of 4 inches, measured from the top flange (Figure 6).

Reusable forms, supported against the lower flange at approximately every three feet, were wired together across the top flange to prevent separation from the steel beam (Figures 7 and 8).

The first layer of reinforcement cage was then welded and placed. Since the transverse steel was not in the form of stirrups it was possible to handle the layers separately, facilitating the placement of the reinforcement. After both layers were in place, they were set on premeasured seats to give them lower and middle clearances and were welded together with steel legs. The seats were then removed. In this manner, it was possible to control the dimensions of the reinforcement in the slab very accurately (Figure 9).

Before casting, the forms were cleaned and oiled with a thin coat of form oil.

2.2.3 Casting When the concrete arrived in a ready-mix truck, it was subjected to a slump test. Upon acceptance it was transferred into a concrete bucket mounted on a fork-lift and taken to the place of casting. There, the concrete was placed in the forms and vibrated with a tube vibrator (Figure 10). Finally the top of the slab was screeded and troweled.

2.2.4 Curing Several hours after casting the concrete was covered with polyethylene sheets. The next day wet burlap was placed over the concrete and again covered. The forms were stripped off after ten days. The slab was kept moist for a period of 28 days and was then allowed to air dry until testing.

2.3 LOADING

2.3.1 Fatigue Loading In order to achieve the objective of the experiment the composite beams were subjected to two kinds of loading: dynamic and static. The dynamic loading was applied by 120 kip, 1100 cycles per second capacity, hydro-electric MTS (Materials Testing Systems) equipment. The system consisted of a compressor, a control panel, two accumulators (line-tamers), and two hydraulic rams with sensitive load cells. The load cells were checked and found to be within one-half percent of the original calibration at all loads. The loads were applied by dialing precalculated settings on the control panel and were read as outputs of the control panel by means of an oscilloscope and two digital voltmeters. Dynamic load was transferred to the beam as a point load at each center span (Figures 3, 11, and 12).

2.3.2 Static Loading Static loading was applied by means of two 200 kip capacity hydraulic jacks. The jacks were calibrated with a 300 kip capacity hydraulic testing machine for their complete range and the calibration was partially checked in a 100 kip capacity mechanical testing machine. The results of the two independent calibrations were within one percent of each other.

In testing, the jacks were connected to an electric pumping system capable of pumping two hydraulic jacks independently. The electric pump was attached by means of two independent lines to two main manifolds. The pressure in the manifolds, which had lines leading to the jacks, was measured by attached pressure cells. These cells enclosed resistance strain gages to which strain indicators were attached. Loading was done by setting the strain indicators to the pre-

calibrated increment of the load desired and pumping until the indicators balanced. The loads were increased and decreased in small increments to insure symmetrical loading. The static load was applied by means of T-shaped distributor beams to produce transverse bending. See Figures 4 and 5 for the static loading arrangement.

2.4 INSTRUMENTATION

2.4.1 Deflection Deflection was measured at midspans with one-inch deflection dials graduated to .001 inches. Both dials were attached to stands which were grouted to the test floor.

2.4.2 Slip The slip between the concrete slab and the steel joist was measured by dials graduated to either .0001 or .001 inches. The slip dials were bolted to brackets, which were then cemented to the inner face of the top flange of the beam with quick drying 910 cement. A stop-angle was then cemented to the bottom of the slab. Finally, an epoxy filler was placed around both the stop and the bracket to further insure a solid connection.

The slip dials were attached to the beam either at the locations of the shear connectors or in the absence of them (NCB6FB1 negative moment region) at the locations of the missing connectors. They were also placed at the ends of the beam and over the center support. At critical points the dials were put in pairs, one on each side of the beam.

2.4.3 Steel Strain Strain in the steel joist was measured by Baldwin-SR4, paper base, resistance strain gages. The gages were attached to the beam in vertical profiles (Figures 1, 2, 13) at predetermined locations and were tested to insure proper operation prior to forming.

The installation of the strain gages was done using the following procedure. First, the beam surface was prepared according to the Baldwin manual (Bulletin 279-B). Then the gages were attached with Nitrocellulose cement and dried under pressure. After twenty-four hours the gages were uncovered, checked, and wired. Finally, they were coated with a rubber-base water proofing compound.

When the water proofing was dry the beam was placed in the testing frame. The strain gages were then calibrated (Figure 14) by loading the steel section to approximately one-half of the theoretical yield stress. The measured strains were compared with those calculated from the elastic theory to determine proper operation of the gages.

2.4.4 Load Cell Testing was done on a two-span continuous beam, making the structure indeterminate. In order to better analyze the system, the center support was made into a load cell to measure the reaction.

The load cell was designed for 320 kip capacity, and was made out of a hollow cylinder, $\frac{3}{8}$ inches thick, 8 inches tall and with an outside diameter of 8 inches. It had 8 resistance strain gages, 4 longitudinal and 4 circumferential, wired into a full Wheatstone bridge.

The procedure of building this load cell is as follows. First, the cylinder was cut to specifications and milled to make the ends parallel. Then a two inch circumferential strip was sanded down to a mirror finish to facilitate the attachment of the strain gages. The locations of the gages were marked carefully and this surface was further improved by means of a metal conditioner and a neutralizer.

They were then placed using 910 cement. The strain gages were first wired individually and were checked for proper operation under a 100 kip capacity mechanical testing machine. After the measured strains proved linear the gages were wired with utmost care into a full bridge. The opposing gages were wired in series, making one of four legs of the full Wheatstone bridge. The cell was checked again to insure proper functioning. Finally, after all connections proved to be satisfactory, a rubber-base water proofing compound was applied gage by gage to eliminate running and spreading.

One-eighth inch deep grooves were machined into two $9 \times 9 \times 1\frac{1}{8}$ inch plates to fit the top and bottom of the cylinder. A third plate was machined to fit a three inch diameter solid cylinder which was to act as a knife edge and was bolted to the top plate. Another plate was machined to fit the solid cylinder to act as a bearing plate between the beam and the load cell. Finally, the cylinder was enclosed in 16 gage galvanized plates, loosely bolted to the top and the bottom plates in order not to carry any load but to protect the inner core of the load cell. The leads from the gages were wired permanently to a jack-plug which was attached to the galvanized plates (Figure 15a, b and c).

The load cell was calibrated three times with a 300 kip capacity hydraulic testing machine and this calibration was checked with a 100 kip mechanical testing machine. The results were within one percent of each other.

The load cell itself was used as the center support. The deflection of this support at maximum load was under .01 inches and was neglected in the analysis.

For the schematic drawing of the wiring of the load cell see Figure 16.

2.5 COMPANION SPECIMENS

2.5.1 Compression Pushouts Nine compression pushouts were cast prior to the casting of the beams. These specimens were tested to determine the fatigue characteristics of the high-strength bolt shear connectors. In keeping with previous studies (4), (5) and (6) all pushouts were built with 8 WF 48, A-36 sections. The drilling of the holes and the placement of the connectors was done in the same manner as for the composite beams. The slabs were 20 inches high by 24 inches wide by 6 inches thick. The reinforcement was again placed identical to the previous studies (4), (5) and consisted of #5 high-strength bars as shown in Figure 17.

Two companion compression pushouts were cast with specimen NCB6FB1. They were identical to the previously cast pushouts except the reinforcement was made into a cage similar to that of the beam slab and consisted of #4 and #5 high-strength bars (Figures 18 and 20). The instrumentation of the compression pushout specimens consisted of four .0001 inch slip dials, one at each of the four connectors.

2.5.2 Tension Pushouts Two companion tension pushouts were cast with composite beam, NCB6FB2. These specimens were similar to the compression pushouts except for their reinforcement, which was made of #4, #5, and #7 high-strength bars (Figures 19 and 20).

In the construction of the pushouts, any mill scale on the steel joist was removed, $\frac{3}{4}$ inch holes were drilled and the connectors were seated similar to the main specimens. The beam stub was then placed in reusable slab forms. The reinforcement was cut to fit the

specifications of the particular set of pushouts, welded together to form a cage or a layer and was placed in the forms. Casting and curing of the pushout specimens were handled similar to the main composite members.

Instrumentation of the tension pushouts required slip dials and strain gages. The slip dials were attached to the joist at the connectors similar to the compression pushouts. To determine the distribution of forces in the specimen, six SR4 resistance strain gages were installed on the three main bars of one of the two slabs. Each bar received two gages at opposing ends of a diameter. The bars were ground to remove all the deformations and sanded down to the required finish. The strain gages were then attached to the bars using quick drying 910 cement. Water proofing compound was applied after the gages were wired and checked.

2.5.3 Concrete Cylinders Three 6 x 12 standard concrete cylinders were cast with each of the nine pushout specimens. Ten cylinders were cast with each of the full scale composite beams which were taken from different sections of the slab as the casting proceeded. Steel molds were used for the cylinders and the casting was done in accordance with ASTM C192-66.

2.5.4 Tensile Coupons Seven tensile coupons were cut from the four foot sections of each of the steel beams that were removed upon their arrival. Two were taken from the top flange, three from the web, and two from the bottom flange. The coupons were standard rectangular coupons. Their dimensions were 18 inches long, one inch wide and the thickness of the material.

2.5.5 Reinforcing Bar Sections Nine eighteen inch long sections were cut from the high-strength reinforcing steel used in the test specimens. There were three sections from each of the different sizes used (#4, #5, and #7).

CHAPTER III

TEST PROCEDURES

3.1 COMPOSITE BEAMS

3.1.1 Preparation of Composite Beams The first step in the preparation for testing was to place the composite beam in the testing frame. Two steel piers 36 feet apart center to center were grouted to the test floor. Rollers were attached to each pier. The composite member was then moved into the frame with the aid of two five-ton capacity pallet trucks and was placed on the supports as a simple beam.

Next the beam was adjusted so that the plane of loading would correspond to the vertical axis of symmetry of the member. Bearing plates were grouted between the steel joist and the rollers to keep the composite member level.

The third step was the placement of the load cell as the center support. The midspan deflection of the member as a simple beam and the strains at six representative points were calculated using elastic theory. The strains at the same points were calculated for a continuous beam. The center of the beam was then raised using screw type jacks until the simple beam deflection and the differences in the strains were cancelled. When the elevation for the center support was determined, the south end of the beam was raised using hydraulic jacks in order to facilitate grouting of the load cell. After the load cell was in place a final bearing plate was installed between the load cell roller and the steel joist and the beam was carefully

lowered onto the screw type jacks which fixed the support elevation. A final reading was taken after setting of this plate and removal of the screw jacks to make sure that the deflection and the strains were in fact within an allowable percentage (2-3%) of the calculated values.

The final step in the preparation of the composite member for testing was the pretensioning of the bolts. The bolts were tightened by the " turn-of-nut " method (9). The bolts were first hand tightened to a snug tight position using a 12 inch crescent wrench. They were then tensioned by an additional half-turn using a larger wrench with an extension.

3.1.2 Preparation of Loading System for Fatigue Loading The rams of the MTS equipment were bolted to the testing frame at the load points prior to the placing of the composite section to facilitate the centering of the member. The rams were leveled and two bearing plates were grouted immediately under them on the slab of the composite member (Figures 3, 11 and 12). These plates were marked in order to detect any horizontal movement during the fatigue loading, which did not occur. The rams and the attached load cells of the MTS equipment were then linked to the master control unit in order to control and monitor the loading.

3.1.3 Preparation of Loading System for Static Loading At the completion of the dynamic loading sequence the MTS rams and the bearing plates on the slab were taken off. Columns, 20 inches in length, were installed at each load point to fill the gap left by the absence of the MTS rams. To these columns 100 ton capacity hydraulic jacks were attached and the load was applied through a T-shaped dis-

tributor beam at each load point to produce transverse bending (Figure 5). The distributor beams were designed to apply 24 kips at the wings of the T and 152 kips at the tail at the maximum load of 200 kips. Bearing plates with dimensions of 12 x 2 x 6 inches were grouted on the slab at the wings under the semi-rollers of the distributor beam and a bearing plate of 8 x 2 x 8 inches was placed at the tail.

Two load points were joined with a longitudinal I-beam (Figure 4) to prevent separation of the jacks as the deflections increased. Seated steel spheres were placed between the jacks and the longitudinal beam in order to transfer the load smoothly. The I-beam was sufficiently reinforced with stiffeners in order to prevent premature failure.

3.1.4 Loading Procedure Prior to the initiation of the dynamic loading, member NCB6FB1 was loaded statically with the MTS equipment symmetrically and unsymmetrically with respect to the interior support up to the working load. During the unsymmetrical loading the south ram was kept at a load which produced a positive south end reaction and the north ram was loaded with increments of 10 kips up to 70 kips. The south ram was then brought to 70 kips with the same increments. During the symmetrical loading both loads were applied simultaneously and slip, strain and deflection readings were taken every 10 kips. The initial static loading of member NCB6FB2 was the symmetrical type of loading only.

At the completion of the initial static testing, the composite members were subjected to fatigue loading. During this process the rams operated in phase with a frequency of 2.5 to 2.7 cycles per

second. For both members the load cycled between 10 and 72 kips, the maximum being the calculated working load for member NCB6FB1. During the dynamic loading phase the operation was stopped at certain increments of cycles and slip, strain and deflection readings were taken at 0 and 72 kip loads. After two million cycles the dynamic loading was discontinued and the composite members were subjected to a final static loading.

Final static loading for both members consisted of increasing the load with increments of 10 kips at both load points up to 200 kips. Readings were taken at each increment after the load was stabilized.

3.2 COMPANION SPECIMENS

3.2.1 Companion Pushouts The nine pushout specimens that were cast prior to the full scale members were tested under dynamic loading, each with varying ranges and a different maximum load. Before testing, the nuts were tightened by the " turn-of-nut " method as previously described. The pushouts were placed on specially cast piers and leveled in a layer of high-strength gypsum plaster. The loads were applied by MTS rams through spherical heads (Figure 22). Prior to the initiation of the fatigue loading, each pushout was loaded statically to the maximum load for the particular specimen at least twice. Slip readings were taken at 10 kip increments. At the completion of the fatigue test, the specimens were moved to a 300,000 pound testing machine and loaded statically to failure. The details and the results of the tests on these specimens are summarized in Tables II and III.

In order to further study the effects of fatigue loading on the bolted connections, one of the two companion pushout specimens (N6F4TB1a) of member NCB6FB1 was subjected to two million cycles of

dynamic loading. Preparation of the pushout for testing was identical to the previous nine specimens. The range of load for N6F4TB1a was determined from a theoretical analysis of the bolts in the slab of NCB6FB1 under the load point at the working load.

After the completion of two million cycles, both companion pushouts were tested in a 300,000 pound hydraulic testing machine until failure. The specimens were leveled on the machine table using a high-strength gypsum plaster and the load was applied through a spherical head onto a distributing plate which was welded to the beam stub. The pushouts were loaded with increments of 10 kips but finer increments were used at critical ranges. For each increment, the load was stabilized while slip readings were recorded. The details and results of these tests appear in Table III.

3.2.2 Tension Pushouts The companion pushout specimens of member NCB6FB2 were cast as tension specimens. They were tested in a confining frame in order to prevent premature separation and twisting of the specimen. The load was applied by a 100 ton hydraulic jack, through a seated steel sphere and a distributing plate which was welded onto the beam stub (Figure 23).

The connectors were pretensioned by the " turn-of-nut " method prior to testing and the pushout was then placed in the test frame. The specimen was leveled and aligned with the aid of four screw jacks and was positioned above the bottom of the test frame with the main bars through the slots that were built into the frame (Figure 23). Steel plates with holes were slipped over the main bars and were welded to the bars to keep the pushout specimen hanging in place from the top of the frame. To simulate the continuity of the reinforcement

in a slab, bar sections were welded from bottom extensions of one slab to the corresponding bars of the other slab. The screw jacks were then removed and the specimen was checked for proper alignment and level.

The load was applied with increments of 10 kips. Cracking and slipping loads were recorded and finer increments were used at critical ranges. At each increment the load was stabilized, while slip and strain readings were taken.

3.2.3 Concrete Cylinders The cylinders were capped with a sulphur compound and were tested in a 300,000 pound hydraulic testing machine.

Of the three cylinders cast with each of the non-companion pushouts, one was loaded to find the compressive strength of the concrete according to ASTM C39-66. The remaining two were loaded to find the modulus of elasticity according to ASTM C469-65, and then continued until failure.

Eight cylinders were cast along the beam and were numbered in order. The odd numbered cylinders were tested at the start of the fatigue loading and the even numbered cylinders were tested after the final static loading. One out of each set was tested according to ASTM C39-66 and the rest according to ASTM C469-65. One cylinder was cast with each of the companion pushouts and was tested according to ASTM C469-65.

All cylinders were tested either during the test or within 48 hours after the completion of the testing of their companion specimens.

3.2.4 Tensile Coupons The steel coupons were tested in a 50,000 pound mechanical testing machine. The exact cross sectional

dimensions of the coupons were determined as an average value of eight different measurements along the length of the coupon. The extensometer used in the testing of the specimens had a gage length of eight inches.

The specimen was loaded to determine its modulus of elasticity, its yield point and its static yield point. The static yield point was found by stopping the testing machine after the yield point had been reached and letting the load reach a stable value (10). This was done three times for each coupon specimen.

3.2.5 Reinforcing Bar Sections The testing of the reinforcing bar sections was done in accordance with that of the coupons, except the static yield was not determined.

CHAPTER IV

RESULTS AND COMPARISONS

4.1 PUSHOUT TESTS

The results expected from the preliminary pushout tests were the development of S-N (stress range vs number of cycles to failure) and load-slip curves for the shear connectors. Although these pushouts were subjected to repeated loading with various stress ranges (Table II), fatigue failure was not achieved. The data therefore, was limited to load-slip curves for the initial static loading up to a predetermined load, cycle-slip curves for the fatigue loading and load-slip curves for the final destructive static loading.

In each loading the slip values were taken as an average of the dial readings, assuming the distribution of load to each bolt was equal. This assumption can be justified since the variation of slip at each connector was relatively small.

The slip that occurred up to a point during loading was recoverable; however, at this point referred to as the " yield point " by Dallam (4), there was a sudden increase in slip with a decrease in load. This jump was due to overcoming of friction between the slab and the joist and was usually accompanied by a loud noise. After the yielding slip the load could be increased, giving another steep section in the load-slip curve until another jump occurred. As the load increased, the intervals between the jumps in slip readings decreased. Until close to the ultimate load, however, the slip occurred in steps (Figure 24),

The results of the pushout tests are shown in Tables II and III. During the initial static testing the pushouts that were subjected to loads of 70 kips or higher had yielding slips at an average value of 18.2 kips per bolt. The corresponding average slip was about .0030 inches.

Since the fatigue loading was done with varying ranges of load, an average value for slip was not detectable; however, all pushouts exhibited an increase in slip during this type of loading. The amount of total slip during fatigue loading was dependent on the range of load, the number of cycles of application and the strength of concrete.

During the final static loading, the pushouts showed similar characteristics as in the initial static loading. That is, audible slips occurred again at about 18 kips per bolt, but the average slip corresponding to this load was .0040 inches. The average ultimate load for the specimens was 34 kips per bolt. The primary failure was apparently caused by yielding of the connectors and excessive local crushing of concrete. In several cases, after the ultimate load had been reached, load application was continued. During this process as the value of slip increased, the applicable load slightly decreased. The secondary failure occurred as shearing of two bolts on the same flange in all cases. An interesting point to note is that the pushouts that were subjected to fatigue loading with maximum load under their cracking load, did not exhibit any cracks during the final static loading, even when the failure occurred without shearing the connectors (Figure 25).

4.2 COMPANION SPECIMEN RESULTS

4.2.1 Compression Pushouts In order to study the effects of repeated loading on the bolted connection, one of the two companion compression pushout specimens cast with NCB6FB1 (N6F4TB1a) was subjected to fatigue loading. It was loaded for two million cycles between 2 and 34.6 ksi per bolt. During the initial static loading of the specimen there was no sudden yielding slip and the average residual slip was under .0006 inches. The repeated loading caused an average residual slip of .0012 inches. The specimen did not exhibit any cracks or other signs of damage throughout the initial two phases of loading.

Both specimens (N6F4TB1a and N6F4TB1b) were then subjected to a final destructive static loading. The fatigue specimen exhibited an average slip of .0021 inches at 80 kips and had an audible yielding slip at 82.5 kips of total load. The average slip corresponding to this load was .0054 inches. The non-fatigue specimen showed .0013 inches of average slip at 80 kips and did not have an audible yielding slip until 113.5 kips. The corresponding average slip for this load was .0061 inches. When the total load reached 140 kips the average slip for the two specimens was .1805 and .0405 inches, respectively. Both specimens started cracking between 180 and 190 kips, but the failure in each case was caused by sudden shearing of connectors and occurred at 200 and 209 kips, respectively (Figure 26). The results for this set of specimens are presented in Table IV and Figure 27.

An interesting point to note is that compared to the non-companion compression specimens the ultimate strength of these pushouts is

about 50% higher. The only real difference between the two sets is in the arrangement and the amount of the reinforcing steel in their respective slabs (Figures 17 and 18). For comparative results see Table III and Figure 24.

4.2.2 Tension Pushouts To study the characteristics of the connection further, two tension pushouts were cast with NCB6FB2. The desired result from these pushout tests was to develop the load-slip relationship of the bolted connection in tension. The results of these tests are summarized in Table V.

In order to be able to detect any eccentricity during the loading of the tension pushouts, the load was also calculated from the strain gages on the main bars of one slab. It was then assumed that the load in the other slab was the difference of the applied and the calculated loads. The load on a connector was taken to be half the value of the load in the slab. In all cases the load-slip curves were derived from the slab of each pushout that received the greater component of the applied load.

The first tension pushout did not have any eccentricity during loading, that is, the calculated load was exactly half of the applied load. The yielding slip occurred at 90.4 kips and was due to cracking of one of the slabs. The cracking of the other slab followed approximately 10 kips later. The pushout failed at 123.6 kips (30.9 kips per bolt) and the failure was caused by splitting of a concrete slab.

The second pushout showed slight signs of eccentricity. Although the applied load was 85 kips when initial cracking and slip occurred, the calculated load was only 40.5 kips for one slab. This left 22.25 kips per bolt for the cracking slab. The second slab cracked after

an increase of approximately 12 kips. This pushout failed by splitting and excessive cracking of the slabs around the connectors and reached the ultimate load at 119 kips (Figure 28). The load that was calculated for the failing slab, however, was 63 kips, that is 31.5 kips per bolt. For the load-slip curves for this set of pushouts see Figure 29, and for typical tension failures see Figure 30.

4.2.3 Concrete Cylinders The results of the cylinder tests for the compression pushouts, companion pushouts and the composite test beams are presented in Table VI. The modulus of elasticity of the specimens was determined from the slope of the stress-strain curves. The compressive strengths and moduli of elasticity that appear in this table are average values.

4.2.4 Tensile Coupons The results of the coupon tests are presented in Tables VII, VIII, IX. All values listed for the flanges and the web are average values of their respective coupons. The last column is the weighted average of the results for the particular specimen. The weighing was done with respect to the measured areas of each section. These values were used in the analysis of the composite test beams.

4.2.5 Tension Bar Sections In order to be able to calculate the distribution of load to the slab of the tension pushouts, strain gages were placed on the main tension bars. Since the placement was done after removing the ribs and decreasing the cross sectional area slightly, a calibration of the stress-strain curve was necessary for accurate results. The results, as calibration curves, were used in the calculations of the load-slip relationships of the tension pushouts.

4.2.6 Reinforcing Bar Specimens The results of the reinforcing bar specimens are presented in Table X. The yield strengths of all the specimens were determined by 0.2% off-set on the stress-strain curves.

4.3 COMPOSITE BEAM RESULTS

4.3.1 General Observations Before the presentation of formal results some observations of the general behavior of the full scale composite members during testing will be summarized.

During the initial static loading of NCB6FB1 the first transverse crack was observed at 40 kips, directly over the center support accompanied by an increase in the deflections of both of the spans and an increase of slip of the non-composite section of the beam. The member was then taken up to 70 kips with increments of 10 kips and was brought back to zero. An average residual deflection of .0077 inches was observed. Residual slip in this case was confined mainly to the negative moment region and the maximum value was .0026 inches.

Next, the composite beam was loaded unsymmetrically as described previously. The unsymmetrical readings caused by the loading in deflection, slip, and strain became symmetrical once the applied P loads were brought to the same value at 70 kips.

At the completion of the initial loading sequence, the member was subjected to fatigue loading. The overall time it took to complete this phase of the experiment was 10 days of continuous cyclic loading with intervals for reading deflection, slip, and strain gages at 0 and 72 kips. During this time it was noticed that the readings of deflection and strain varied without an obvious pattern and without any corresponding change in slip. It was assumed that this be-

havior of higher or lower readings compared with the previous ones was mainly due to temperature and humidity changes in the laboratory from one interval to the next.

Two more transverse cracks were observed about 6 inches on either side of the first crack during the early phases of the fatigue loading, at about 28,000 cycles. The slip readings increased until the count of 400,000 cycles and stopped except for some irregular small increases throughout the rest of the dynamic loading. The substantial increases (over .0010 inches) were limited to the negative moment region. The maximum value of residual slip during this phase was .0018 inches. The residual deflection readings, although irregular, had an increasing pattern. The total change in the readings at the end of the fatigue loading was .0102 inches. Extensive branching out of the initial cracks was observed during this phase.

At the end of the fatigue loading sequence, the loading apparatus was changed and the member was subjected to a final static loading. During this loading two more transverse cracks, at about 7 inches from the previous cracks, were observed between the loads of 110 and 120 kips. The slips (audible) corresponding to these loads were much larger throughout the beam, with maximum values of .0100 inches for the composite and .0120 inches for the non-composite sections. At 150 kips, longitudinal cracks due to transverse bending and the cracks in the slab under the load points were observed. As the load was increased there was an apparent branching out of the transverse cracks over the negative moment region accompanied by several more independent transverse cracks. Also the cracks under the load points propagated higher in the slab.

The width of the initial crack was measured at 70, 90, 120, 150, and 200 kips. The readings in millimeters were .20, .24, .30, .36, and .46 (.0079, .0092, .0118, .0142, and .0181 inches respectively). The width of the initial crack at the interior support was the maximum throughout the experiment.

Member NCB6FB2 had its initial transverse crack at 40 kips directly over the center support. The second transverse crack was observed about 15 inches south of the initial one at 70 kips. There was a noticeable increase in the deflection at the occurrence of each crack, however, the accompanying slip readings did not change considerably. The average residual deflection was .0112 inches and the maximum residual slip observed was only .0007 inches.

The width of the initial crack was measured at 50, 60, and 70 kips during the initial static loading. The corresponding values were .20, .27, and .32 millimeters (.0079, .0106, and .0128 inches respectively).

During the very early phases of the fatigue loading of NCB6FB2, at approximately 4000 cycles, a third transverse crack about 9 inches north of the initial one was observed. There was no branching of cracks throughout the dynamic loading of the member. At the completion of two million cycles, the member exhibited .0099 inches of average residual deflection and the maximum value of the residual slip along the beam was .0006 inches.

The fatigue loading lasted nine days and the effects of temperature changes were noticeable in the behavior of NCB6FB2 strain and deflection readings.

During the final static loading the audible slip with an increase

in the gage readings occurred at 130 kips. At this load longitudinal cracks due to transverse bending were observed. Also two independent transverse cracks were formed about 8 inches either side of the initial center crack. They had propagated the full width of the slab at about 150 kips. At this load two more transverse cracks were observed about 40 inches from the first crack. The first transverse crack under the load points was observed at 170 kips. During the rest of the final static loading there was very little branching out of the cracks. Only very short new cracks formed in the negative moment region, independent from the existing ones.

The width of the initial crack was measured at 70, 100, 130, 150, 170, and 200 kips. The readings were .32, .40, .46, .58, .70, and 1.0 millimeters (.0128, .0157, .0181, .0228, .0276, and .0394 inches respectively).

There were no noticeable effects on the connectors of both of the composite members. All the connectors were fully intact at the end of each test.

4.3.2 Analysis In all the theoretical and experimental calculations the actual beam measurements (Table I) and the information obtained from the cylinder (Table VI) and the coupon tests (Tables VII-X) were used. The properties of the steel joist varied for the top flange, web, and bottom flange. This fact was considered in the transformations for the calculations of the centroid depth, moment of inertia and also in the determination of the stresses and strains.

The internal couple method was used for the calculations of the moment capacity of the section for a given criteria, such as the working or yield capacity. For member NCB6FB1 the moment of inertia cal-

culations were based on no interaction for 52 inches on either side of the center support, that is up to the effective area of the first bolt. It was also assumed that the curvature of the two components were equal at any load (11). For sections between the contraflexure points, the part of the slab in tension was considered cracked, and for the sections between the contraflexure points and the first bolts, the full slab was taken into account. For the bolted sections of the test beam, the moment of inertia was determined for a composite section using section transformations (12).

For the theoretical working and yield capacities of member NCB6FB1, the strains in the bottom of the lower flange over the center support were the controlling conditions. The moment capacity for this critical condition was calculated by means of the internal couple method and the assumption of identical curvature was taken care of using :

$$M_{\text{section}} = \left\{ 1 + \frac{(E_{\text{slab}})(I_{\text{slab}})}{(E_{\text{beam}})(I_{\text{beam}})} \right\} M_{\text{beam}}$$

The theoretical ultimate capacity of the section was determined using ultimate strength theory (13) for the slab and the assumption that all the steel had yielded at the failure of the critical cross section. Curvature for the beam and the slab was therefore assumed different and separation during testing confirmed this assumption.

For member NCB6FB2 the moment of inertia calculations were based on full composite action and the theory of transformed sections throughout the beam. The slab for the sections between the contraflexure points was assumed fully cracked.

The theoretical working, yield and ultimate moment capacities

for NCB6FB2 were calculated by means of the internal couple method. The theoretical working capacity criteria was taken to be the critical strain under the bottom flange over the center support, although the reinforcement at the same cross section reached this strain earlier. The difference was under 6% of the assumed moment capacity. This was done in order to be able to compare the theoretical values with the experimental capacity, since there were no strain gages on the reinforcement. The theoretical yield capacity was based on the first yield of any steel in the cross section and was controlled by the strain under the bottom flange at the same cross section. In the calculations of the ultimate moment capacity for NCB6FB2 the assumptions were that all the steel had yielded and that no part of the steel had reached strain hardening.

Using the calculated properties of the composite sections the analysis for all loads were then carried out by means of a computer program using the stiffness method for a variable EI along the beams. Using theoretical symmetry the beams were analyzed as propped cantilevers, working only with the right span of the continuous sections.

For the experimental working and yield loads of both the members, the allowable strains were first calculated for the steel in the cross sections that could possibly control the load. The controlling cross section was then picked and the accompanying strain was compared with the data obtained from the strain gages. In doing so the dead load strains were also taken into consideration. Whichever strain reached the value of the calculated working or yielding strains, the load at which these strains occurred was denoted as the working or

yield loads. There was no collapse since a mechanism had not formed although a plastic hinge formed over the center support in NCB6FB1.

The results of the theoretical and experimental analyses for members NCB6FB1 and NCB6FB2 are listed in Table XI.

4.3.3 Deflection Results The deflections for both members are presented in Figure 31. The deflection points plotted are the average of both spans directly under the load. The solid lines included in the figure are the theoretical full interaction and no interaction deflections, and were calculated using the stiffness method and variable EI .

The deflections of NCB6FB2 are slightly higher than the theoretical full composite deflections, while member NCB6FB1 obviously developed some composite action due to the restraint of the connectors in the positive moment region.

4.3.4 Slip Results The slip distribution along the members are shown in Figures 32, 33, 34, 35, and 36. The distribution is plotted for the working and yield loads of NCB6FB1, working and yield loads of NCB6FB2 and at 200 kips in a comparative manner. The slip for a given load is plotted against the distance from either side of the center support for the full length of the composite members. The arrows marking the direction of slip in the figures show the direction of slip of the slab with respect to the steel joist. As seen from the figures the slip is zero under the load points and over the center support and the slab moves away from the load points.

It can also be seen from the figures that the lack of composite action over the negative moment region seems to affect the bolted sections throughout the beam. While the slip for NCB6FB1 is much high-

er in the negative moment region as expected, it is also higher in the composite positive moment regions, indicating that the connectors carry more force than what is predicted by elementary beam theory.

4.3.5 Reaction Results The results of the reaction measured from the load cell are plotted against the applied load for both composite sections (Figure 37). In order to be able to use a larger scale only half of the numerical value of the reaction is used, which is actually the shear force at the center support.

For both members the measured reactions are only slightly higher than those calculated theoretically with the maximum difference less than 2% of the measured reaction.

4.3.6 Strain Results The strain profiles are presented next (Figures 38, 39, 40, 41, 42, and 43). These profiles are taken from representative sections of the beam: Section A directly under the load; Section B in the positive moment region 68 inches from the center support; and Section C in the negative moment region 35 inches from the center support. They are plotted against the depth of the member and a positive strain indicates tension.

The profiles are plotted for the working and yield loads of NCB6FB1 and working and yield loads of NCB6FB2 in a comparative manner, that is, each figure shows the strain profile across a given section of both beams at two given loads. The theoretical profiles are shown by solid lines and the experimental values are plotted using a different symbol for each of the cases.

The theoretical strains were calculated by using the measured reaction to reduce the system to a determinate structure and applying elastic beam theory.

The theoretical values of strains at Section A (under load) generally show good agreement with the experimental strains. The assumptions (full composite action) used in the calculations of the theoretical values seem to be justified. However, the theoretical strains differ considerably from the experimental values as the profiles approach and enter the negative bending region. This region is also the section of the beams where the maximum slip occurs. The effects of slip on the discrepancy between the experimental and the theoretical strains is especially obvious at Section B (68 inches from center support). In the calculations of the theoretical strain values for NCB6FB1, full composite behavior is assumed since there was connection between the slab and the joist on both sides of the profile. The slip values at this section, however, are about 80% of the maximum slip throughout the beam. Thus, the differences in the theoretical and experimental strains could in large part be due to the presence of slip at this section. The theoretical and experimental values of strain for NCB6FB2 at Section B, on the other hand, show generally good agreement. It should be noted that the slip for NCB6FB2 in this region is approximately 30% of the slip in NCB6FB1.

The behavior of the profile 52 inches from the center support, which is not plotted in this report, could not be accounted for. This profile showed signs of faulty gages and did not plot in a straight line, with deviations as high as 100%. This behavior was noticed in the testing of both beams and is especially obvious as the contra-flexure points extend closer to this region.

The theoretical strains at Section C (35 inches from center

support) differ from those obtained experimentally. The assumption of fully cracked section in the calculation of the theoretical values results in a lower neutral axis for these values. As the load increases the experimental neutral axis seems to approach the calculated values due to the cracking of the slab over this region. The force in the slab of NCB6FB1 at Section C, that causes slip, is relatively smaller than the force at Section B, which causes the same amount of slip since there are connectors on both sides of Section B. Therefore, although considerable slip is present in this region - as much as at Section B - it does not seem to affect the position of the neutral axis as much as at Section B.

4.4 COMPARISONS

4.4.1 Cracking Patterns For both composite beams the first transverse crack was observed at 40 kips of applied load. NCB6FB1 did not exhibit any additional cracks during the initial static loading, while NCB6FB2 showed another transverse crack, as previously described, at 70 kips. This fact was attributed to the stiffer behavior of the second beam in its negative moment region.

During the fatigue loading phase, NCB6FB1 cracked readily, in the form of independent transverse cracks and also extensive branching out of the already present ones throughout the negative moment region. On the other hand, NCB6FB2 exhibited only one additional transverse crack, as described before, and only small extensions of the original cracks were noted.

The cracking pattern of NCB6FB1 throughout the final static loading was closer to the assumption of a fully cracked section with extensive branching of cracks. There was no uncracked section of slab in

the negative moment region, with any substantial length, at a load of 150 kips. NCB6FB2, however, exhibited only five main transverse cracks, with little branching until 150 kips. All transverse cracks of the second beam, with the exception of the middle one, started in the vicinity of a shear connector under the slab. For the negative moment region cracking patterns see Figures 44 and 45. Also to aid the comparison of the behavior of the members with respect to their cracking patterns, comparative sketches of the negative moment region are included (Figure 46). These sketches are of the cracking patterns at the working and yield loads of the respective members during the final static loading and at the final load of 200 kips. It is of interest to note that NCB6FB1 (no connectors) had numerous cracks of relatively small width whereas NCB6FB2 had fewer and wider cracks.

The longitudinal cracking patterns under the load points were identical for both composite members. They appeared as a single crack, increasing in length on both sides of the load points, as the load was increased. (Figures 47 and 48).

The flexural cracking patterns under the load points (positive moment region) were also similar. The first cracks for NCB6FB1 were observed at a load of 150 kips, while NCB6FB2 did not exhibit the same until 170 kips. At the end of the final static testing the penetration of flexural cracks for NCB6FB1 were measured to be higher in the slab than those of the second beam. (Figures 49 and 50). These facts were also attributed to the stiffer behavior of NCB6FB2 in the negative moment region.

4.4.2 Beam and Companion Pushouts The load slip results of the companion pushouts were to be compared with that of several connectors

in the full scale members. The strain observed from the vertical profiles was integrated over the area of the beam and the result was multiplied by the experimental modulus of elasticity giving the axial force in the beam. The difference of forces between the profiles was to be assumed as the shear carried by a pair of connectors.

Unsatisfactory behavior of the central profiles (52 inches from center support), however caused the calculations to be inconsistent and unworthy of presentation. Therefore, no attempt was made to compare the load-slip relationships of the composite members with that of their companion pushouts.

4.4.3 NCB6FB1 and NCB6FB2 Throughout this report the results were presented in a comparative manner, with data for both of the composite sections appearing in the same figure under similar conditions.

In comparing the members for stiffness from the deflection curves, reaction results, and the cracking patterns it can be seen that member NCB6FB2 - with connectors over the negative moment region - was considerably stiffer over this section. At 200 kips of applied load, the negative moments for NCB6FB1 and NCB6FB2, calculated from the measured reactions, were 5687 and 6324 inch-kips respectively. It can be said, then, that NCB6FB2 behaved 11% stiffer with respect to negative moment over the center reaction. The moments that were calculated from the measured reactions versus applied load are plotted in Figure 51, for a further comparison of the behavior of the two members.

The behavior of the members with respect to slip can readily be seen from the slip distributions. The slips at the bolt 59 inches from the center support (first bolt for NCB6FB1 into the span) for

both beams are plotted to show the typical slip differences for the beams for the full load range (Figure 52). It is apparent that in composite beams without shear connectors in the negative moment region, the connectors adjacent to this region will be subjected to considerably more shear force than predicted by elementary beam theory.

It is of particular interest to note that the presence of bolt holes in the tension flange over the center support of beam NCB6B2 did not in any observable way adversely affect the behavior of this beam during either the fatigue or static loading. This was due to the fact that friction was not overcome in the connection during the fatigue loading.

CHAPTER V

SUMMARY AND CONCLUSIONS

5.1 SUMMARY

Nine pushout specimens were tested to determine the fatigue characteristics of the high-strength bolted connection. The data used in the investigation was load-slip and cycle-slip curves.

Two double span continuous composite members were tested using dynamic and static loading, to determine the effects of fatigue loading on the static behavior of the composite members. Both members were designed according to AASHTO specifications with only one using $3/4$ inch bolted shear connectors over its negative moment region.

Load-deflection, cycle-deflection curves, strain profiles, slip distributions for dynamic loading, slip distributions for static loading, and load-reaction curves for the interior support were used in the investigation of the behavior of the full scale composite members. Predicted loads, deflection, and reactions were compared with the actual values obtained during testing. Using the above mentioned data, the behavior of the two composite members and their cracking patterns were compared.

Two compression and two tension pushouts were tested. One compression pushout was subjected to fatigue loading prior to destructive static loading. Load-slip curves and ultimate strengths were investigated.

5.2 CONCLUSIONS

The following conclusions were drawn from this investigation:

1. The magnitude of the critical or yield load and the

ultimate load for pushout specimens subjected to fatigue loading (up to 10 million cycles) was essentially the same as those for pushout specimens subjected to static loading.

2. The magnitude of the ultimate load for pushout specimens with two layers of reinforcement in the slabs (Figure 18) was 50% greater than the average ultimate load for pushout specimens with one layer of reinforcement in the slabs (Figure 17). The critical or yield load was not affected by the presence of additional slab reinforcement.
3. The member with shear connectors over its negative moment region exhibits practically no slip in this region at its working load compared with the member lacking such connectors.
4. The absence of shear connectors in the negative moment region increases the slip and connector force in the positive moment region.
5. The elimination of the shear connectors over the negative moment regions reduces the working and the first yielding loads of a continuous composite member by 30% and 20%, respectively.
6. Elementary beam theory (assuming complete interaction) can satisfactorily be used to predict the behavior of a continuous composite member up to its yield load provided sufficient connection exists and careful consid-

eration is given to slab cracking in the negative moment region.

7. There are fewer cracks (but of greater width) when connectors are placed in the negative moment region.
8. Fatigue is not a factor in the design of composite members using high-strength bolts as shear connectors.

There were six major objectives of this study which are listed on pages 6 and 7. Objectives 1, 3 and 4 were discussed at length and conclusions regarding them have just been stated. Objective 2 was to determine if the fatigue behavior of the bolts in the pushout tests could be used to predict their fatigue behavior in the beam. Objective 5 was to determine the range of load that would cause fatigue failure. Since fatigue failure was not attained for loading at or below the critical load of the bolts, and since the design load for a connector would be based upon a factor of safety applied to the critical load, these objectives were accomplished in that they were not applicable because the fatigue behavior was approximately the same as the static behavior.

Objective 6 was to determine the effects of longitudinal slab cracking on the connector behavior and although cracks did appear (Figures 47 and 48) there was no apparent effect upon the connectors. It could have been a factor if the static loading could have proceeded to develop the ultimate moment capacity in the positive moment regions.

FIGURES

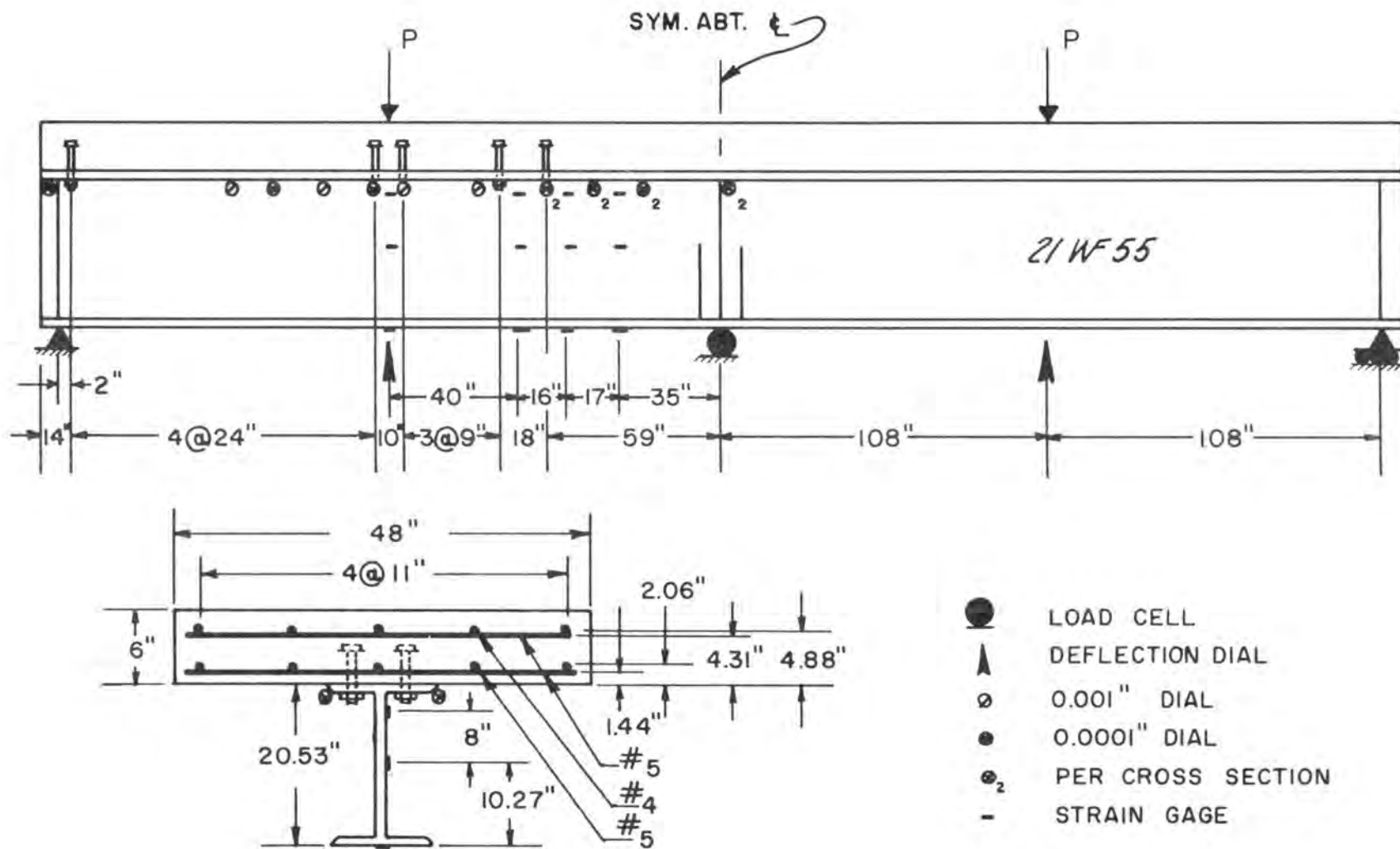


Figure 1 Dimensions and Instrumentation of NCB6FB1

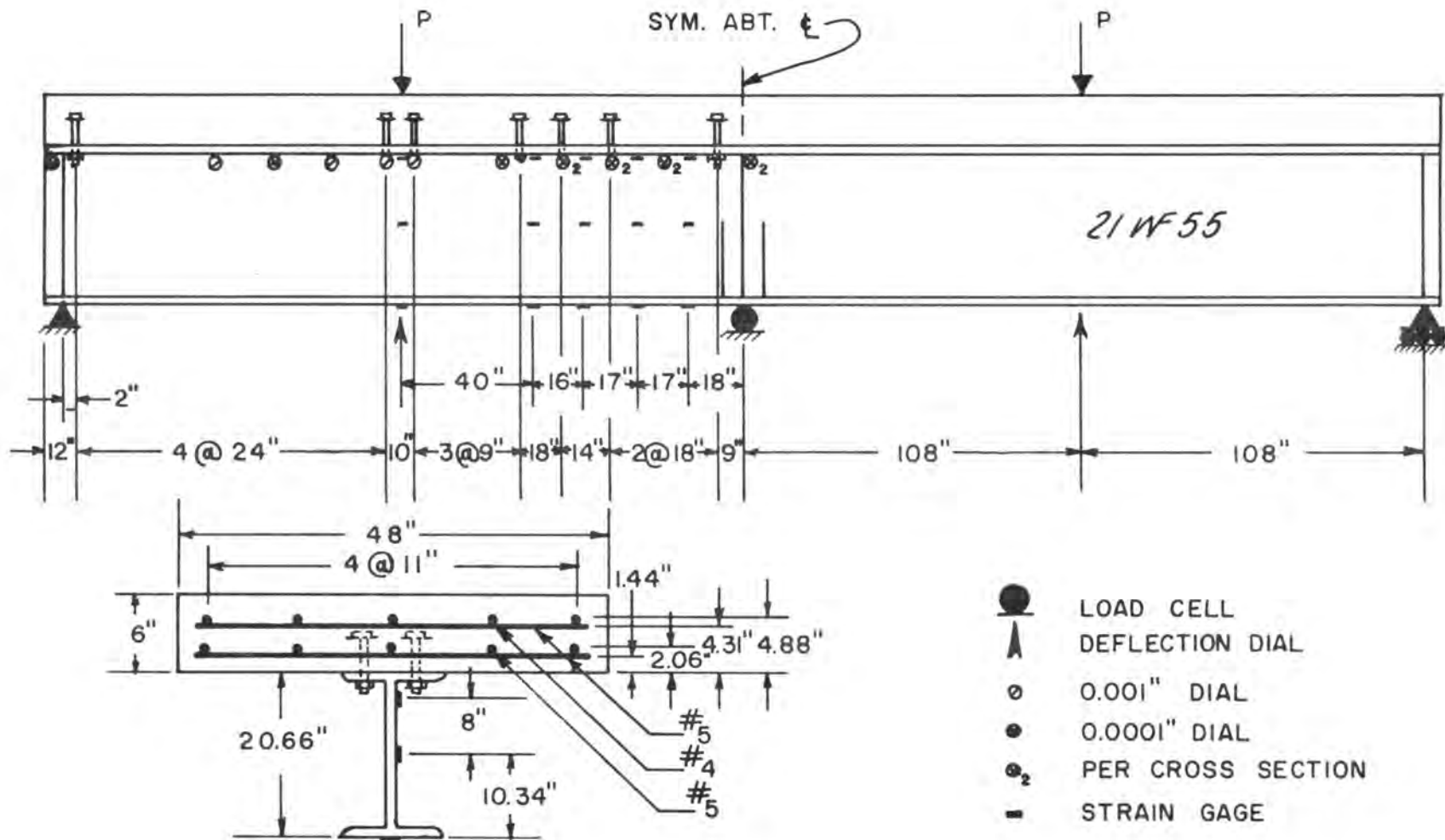


Figure 2 Dimensions and Instrumentation of NCB6FB2

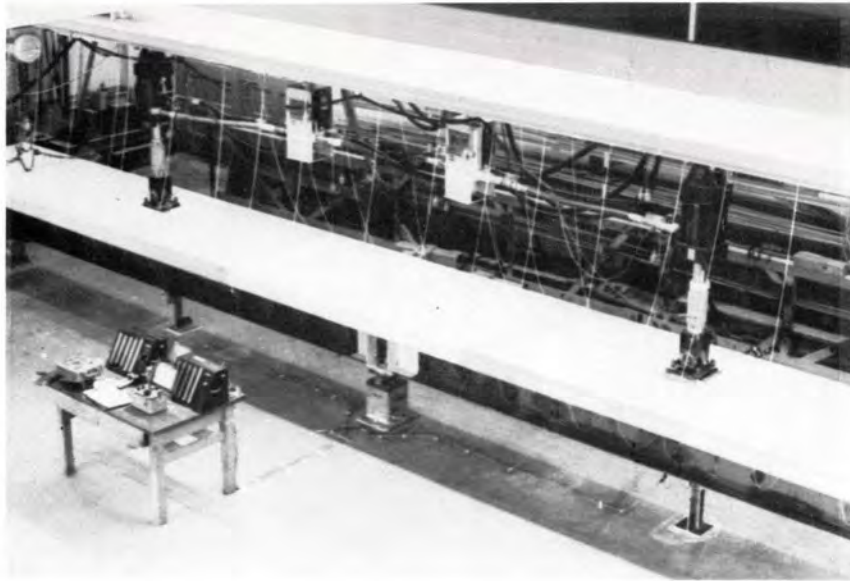


Figure 3 Dynamic Loading Apparatus

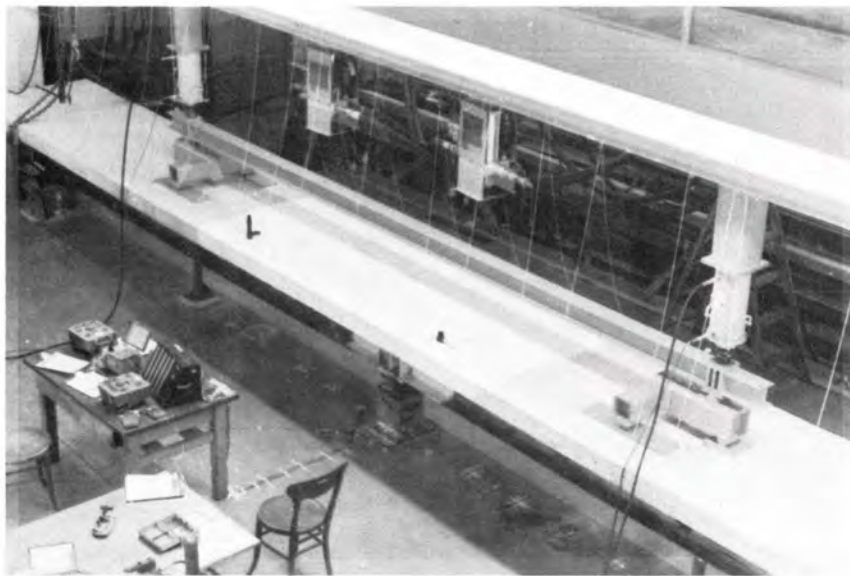


Figure 4 Static Loading Apparatus

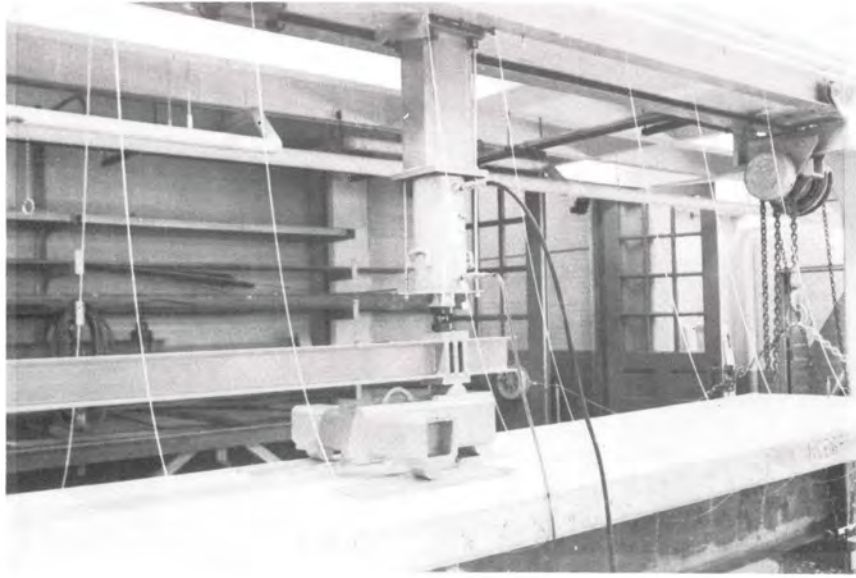


Figure 5 Static Load Point

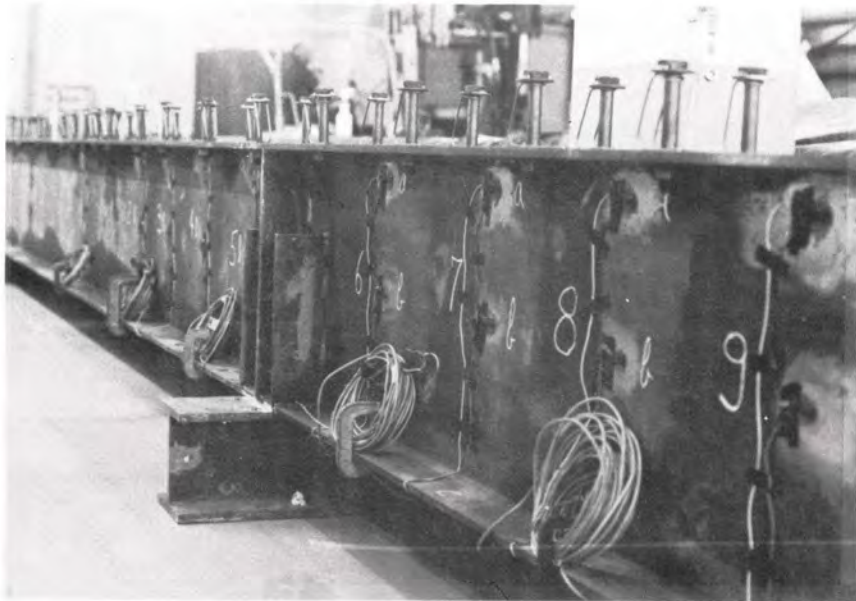


Figure 6 Placement of Bolts

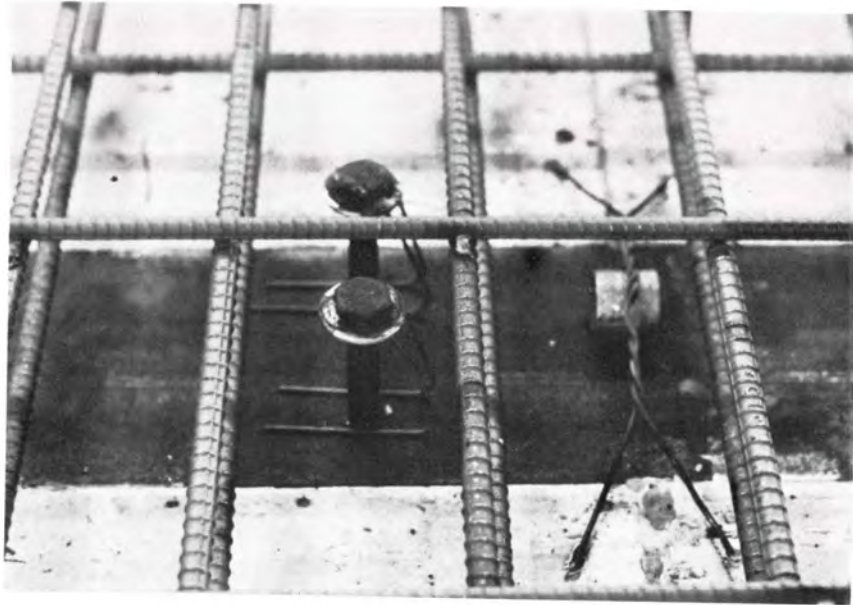


Figure 7 Wired Forms



Figure 8 Supported Forms



Figure 9 Reinforcing Cage



Figure 10 Casting

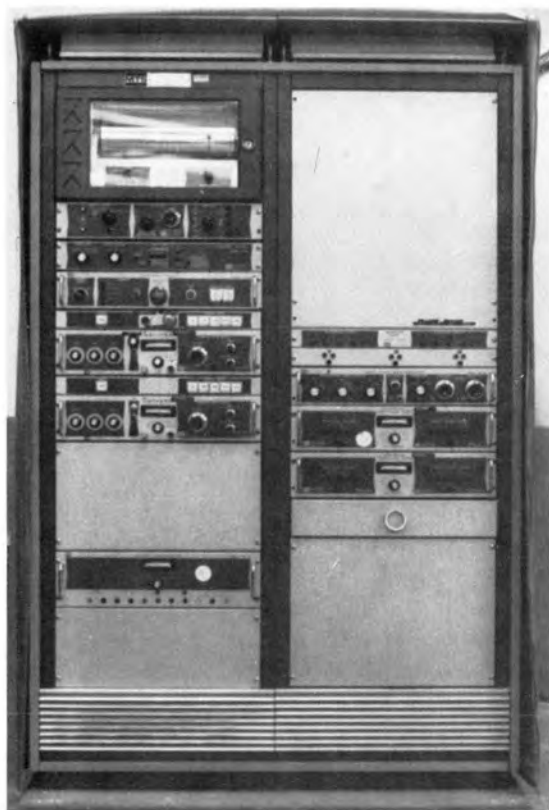
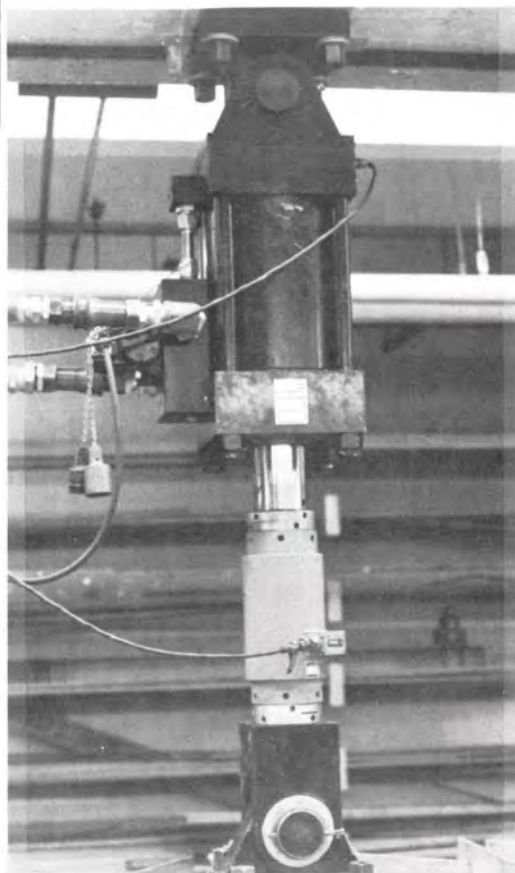


Figure 11 MTS
Control
Panel

Figure 12 MTS Ram



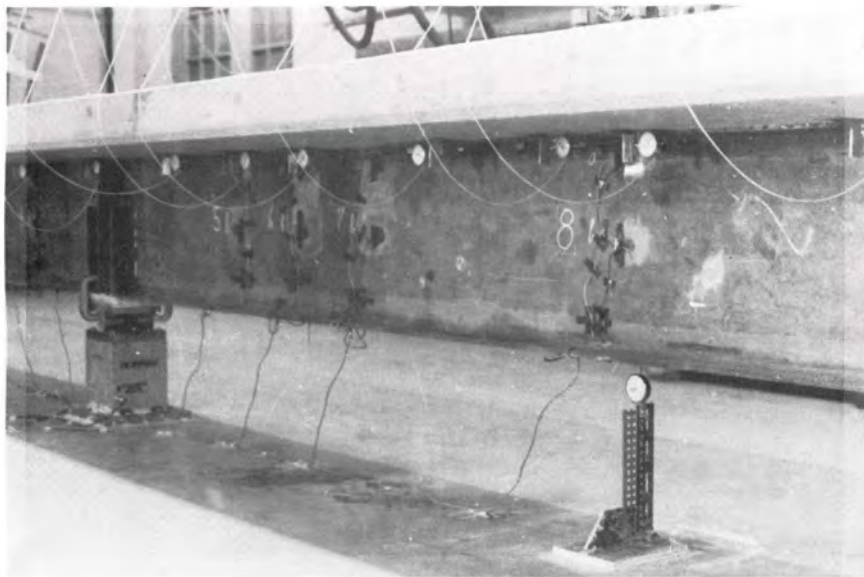


Figure 13 Instrumentation

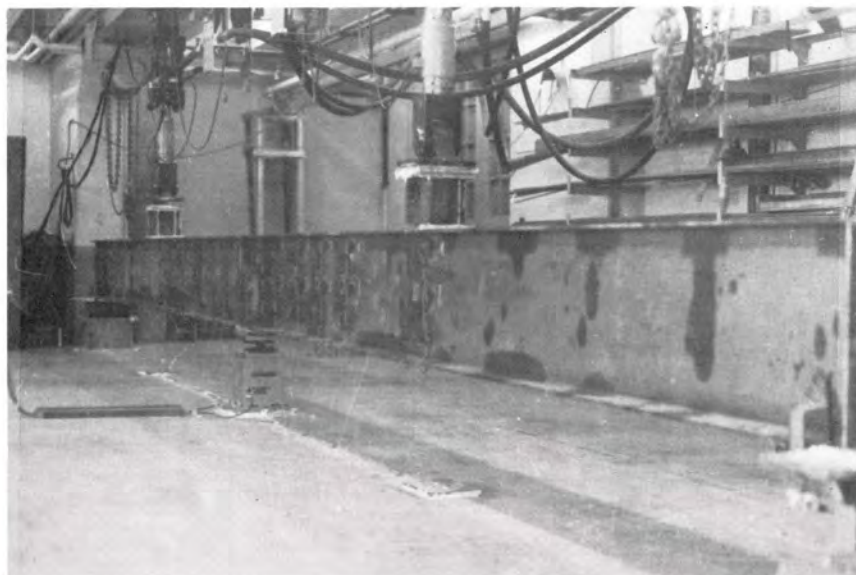


Figure 14 Strain Gage Calibration

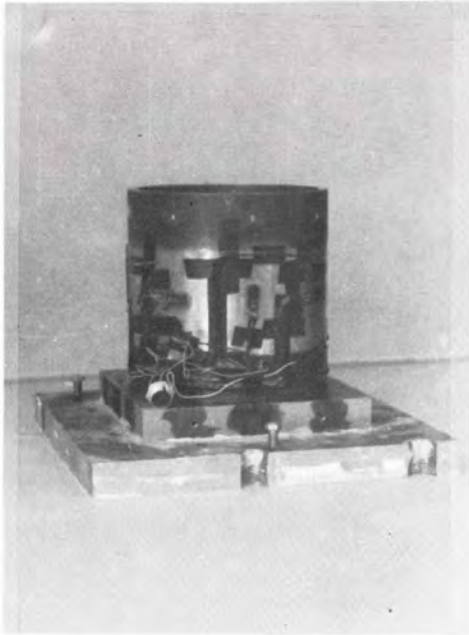


Figure 15a Load Cell Core

Figure 15b Load Cell
as Support

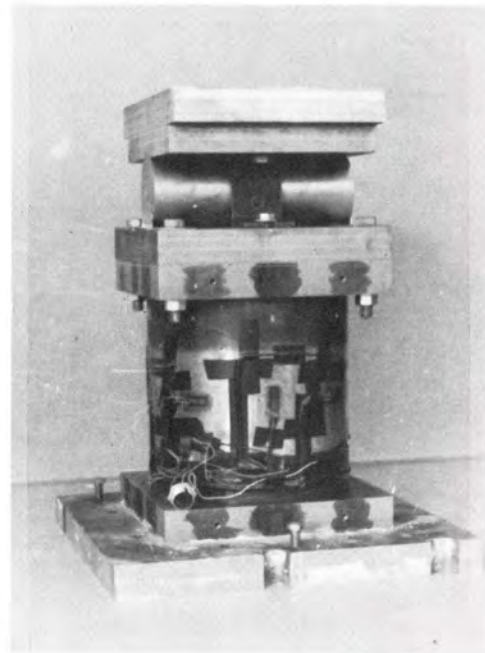
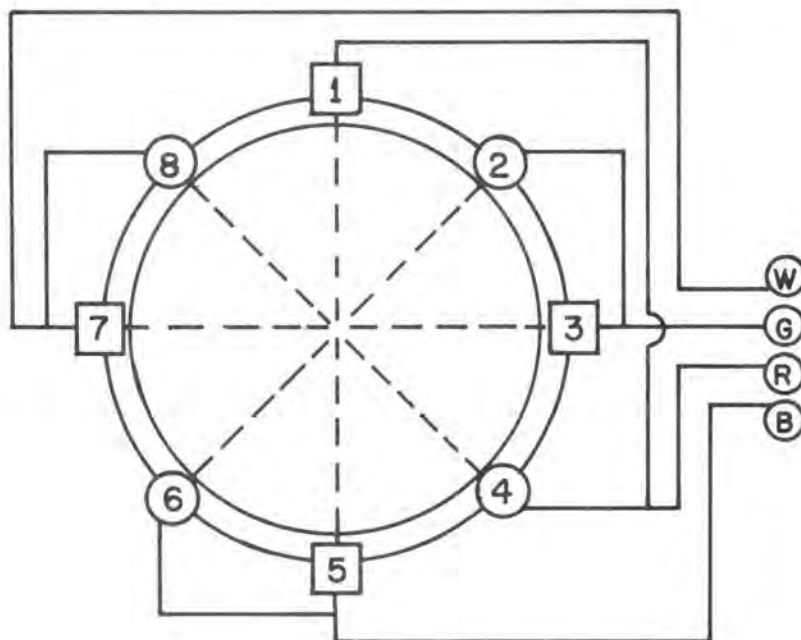
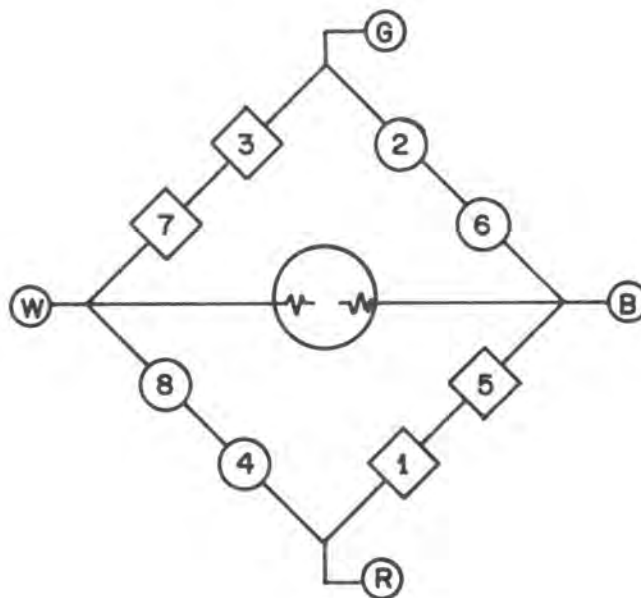


Figure 15c Load Cell
Ready to Use



ACTUAL



SCHEMATIC

Figure 16 Load Cell Wiring

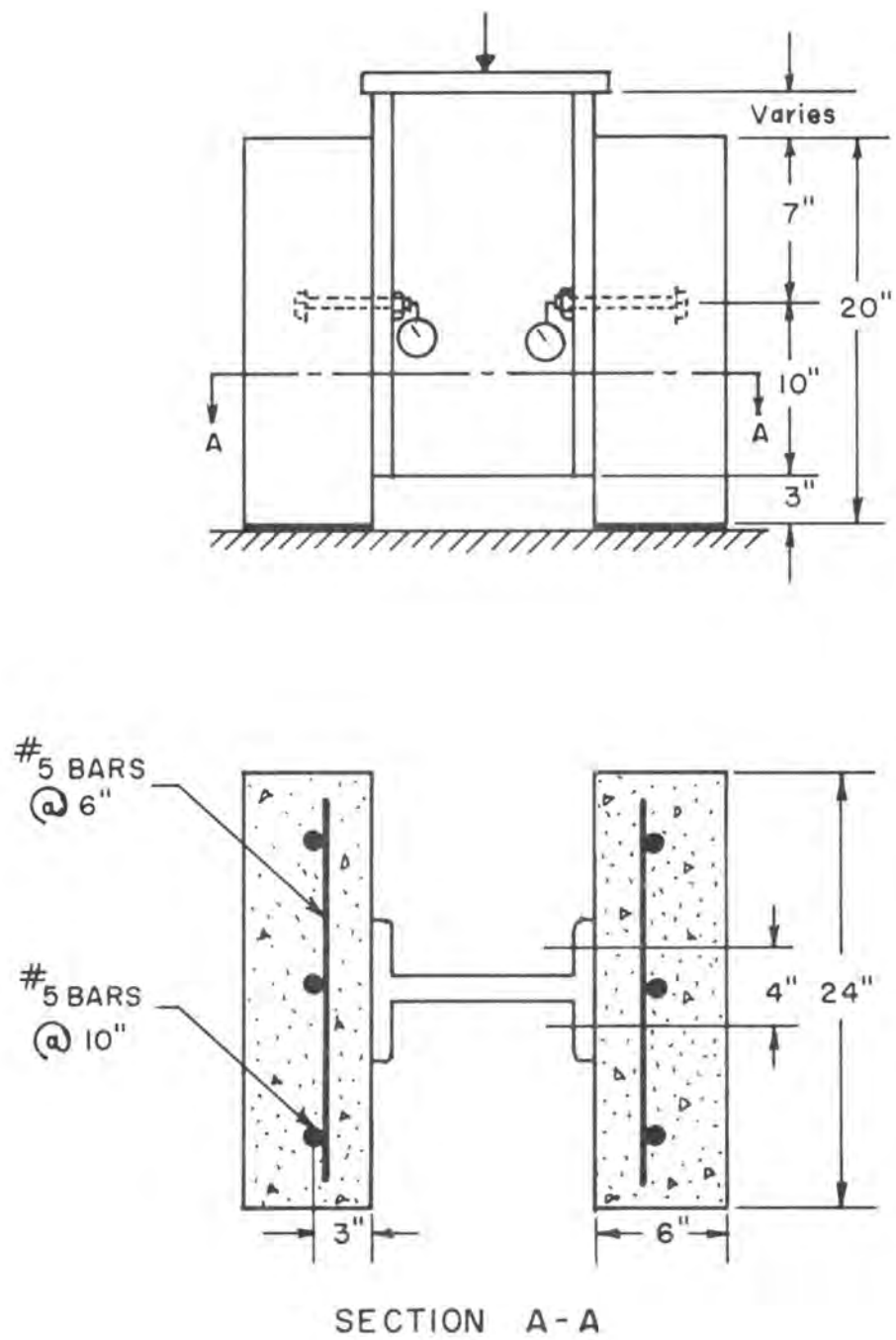


Figure 17 Fatigue Pushout Specimen

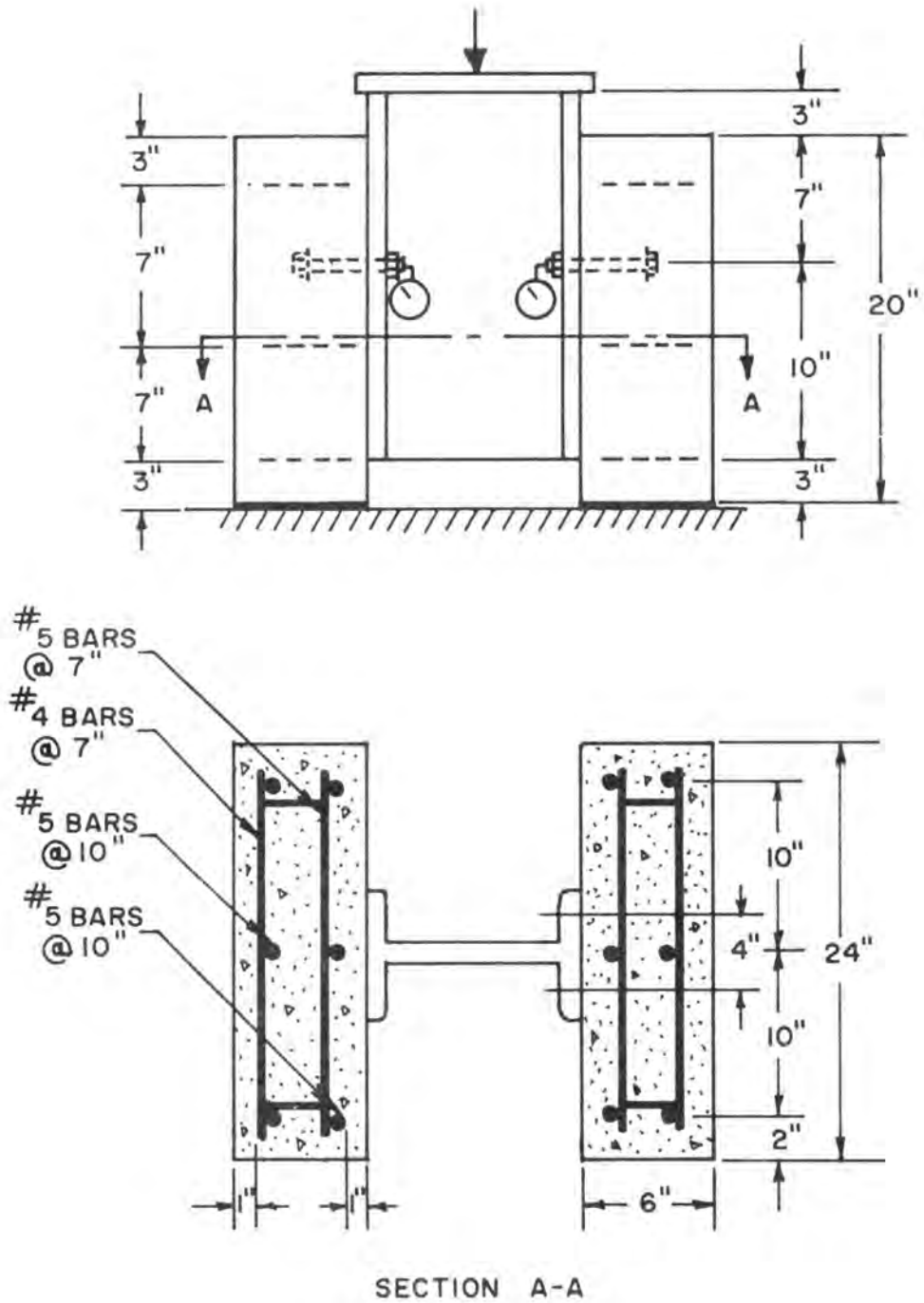


Figure 18 Beam Companion Compression Pushout Specimen

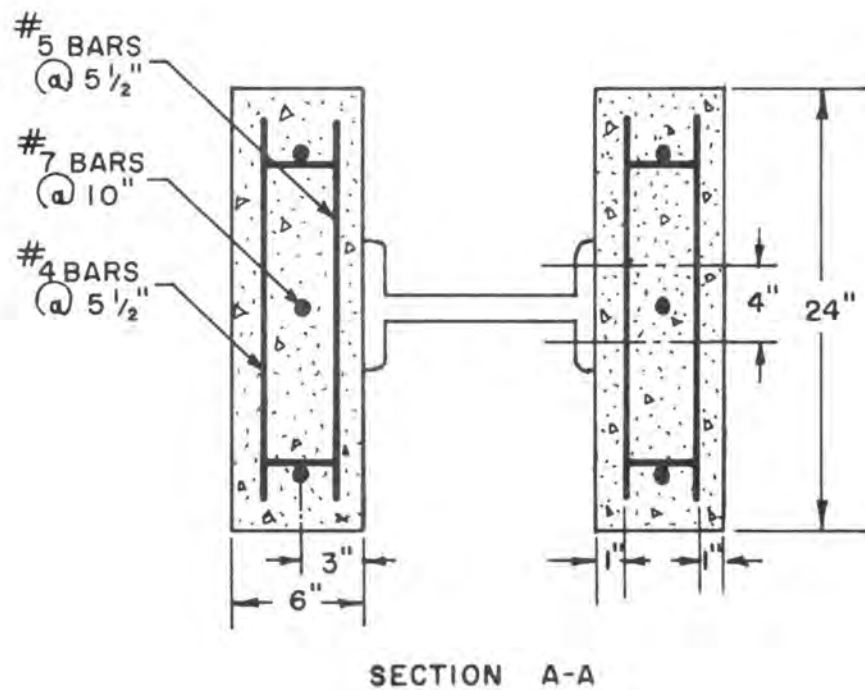
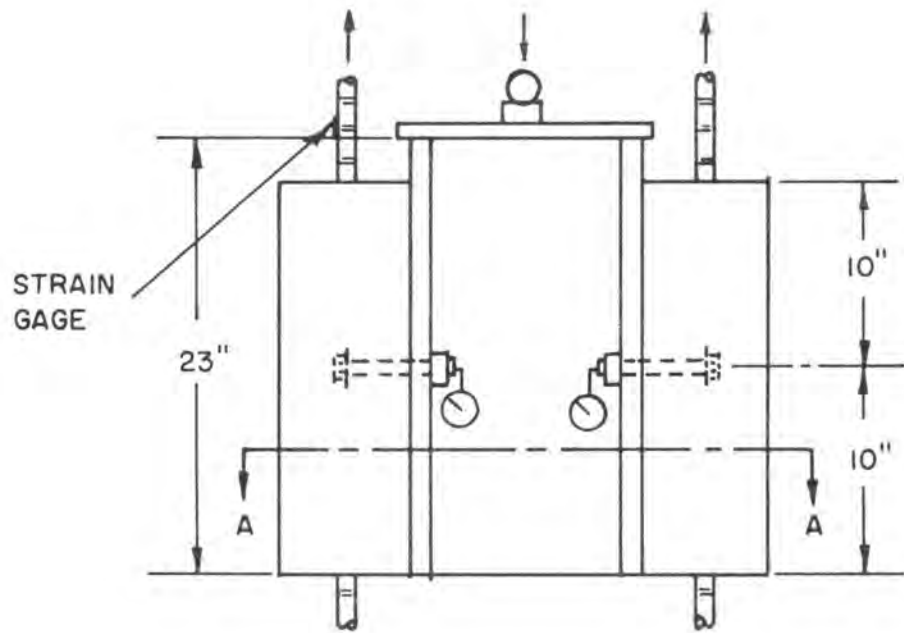


Figure 19 Companion Tension Pushout Specimen

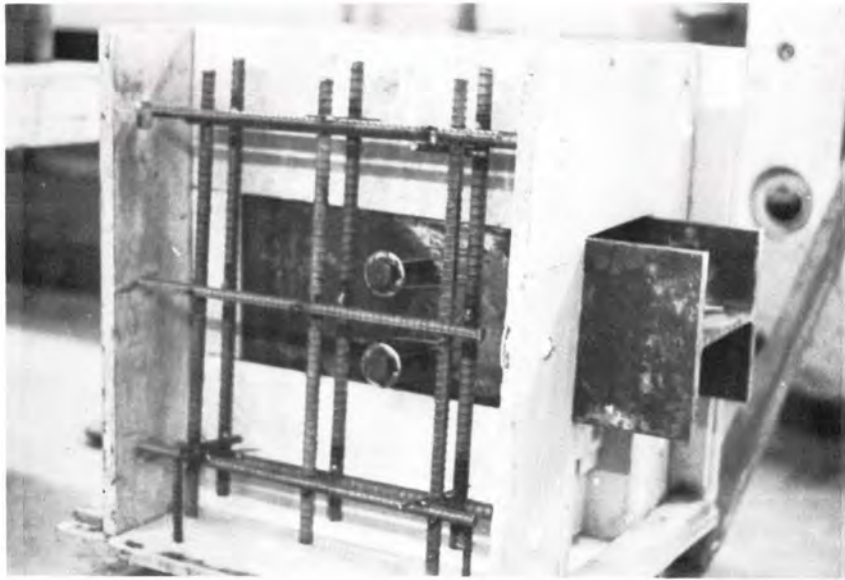


Figure 20 Reinforcing - Companion Compression Pushouts

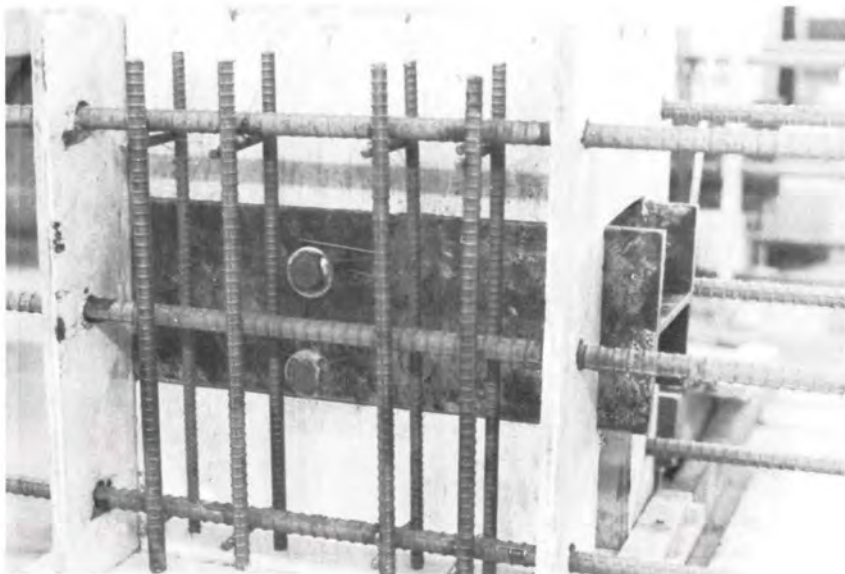


Figure 21 Reinforcing - Companion Tension Pushouts



Figure 22 Fatigue Tests on Pushouts

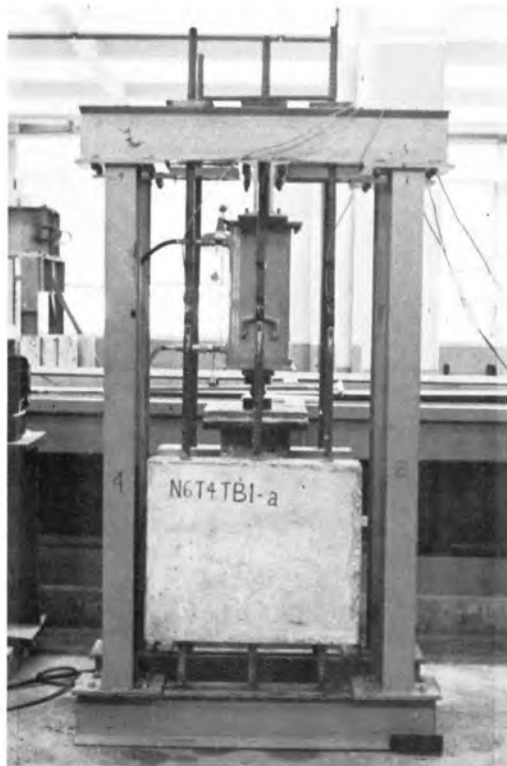


Figure 23 Tension Test on Pushouts

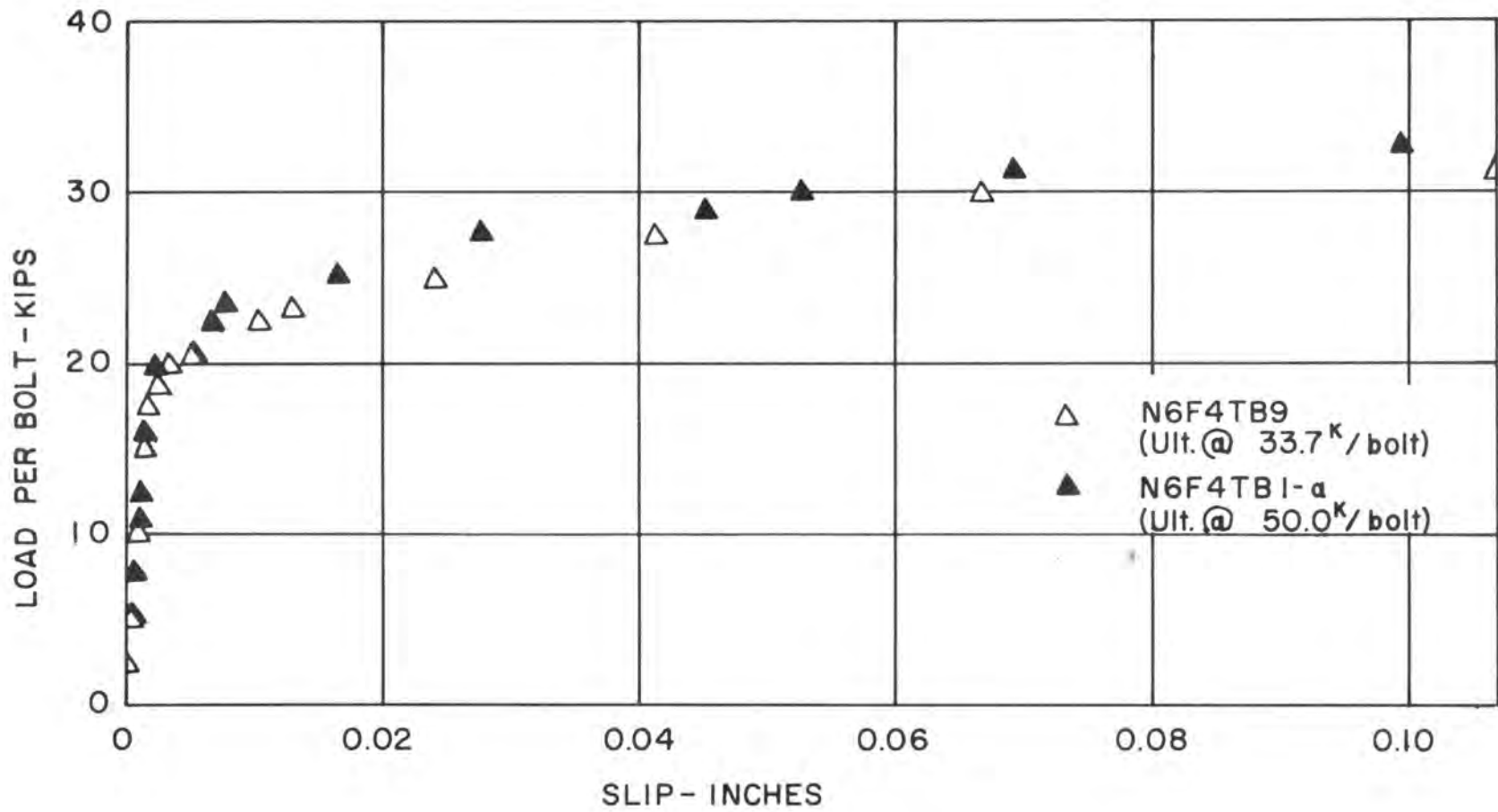


Figure 24 Load-Slip Comparison of Non-Companion and Companion Pushouts

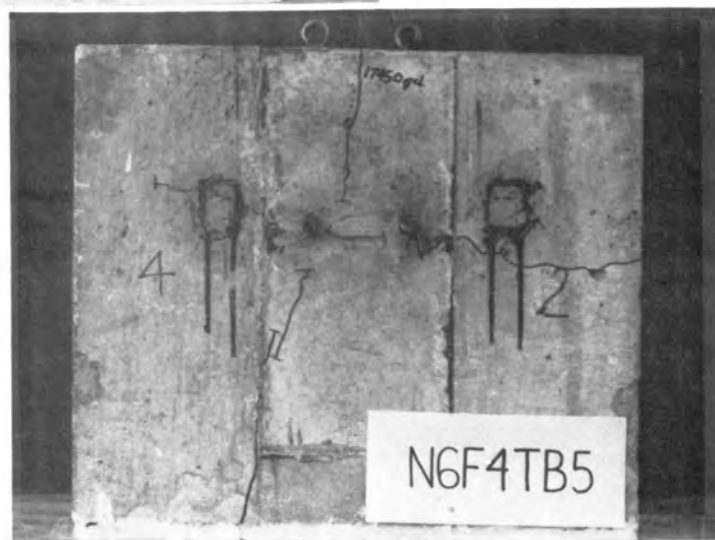


Figure 25 Non-Companion Compression Pushout Failures

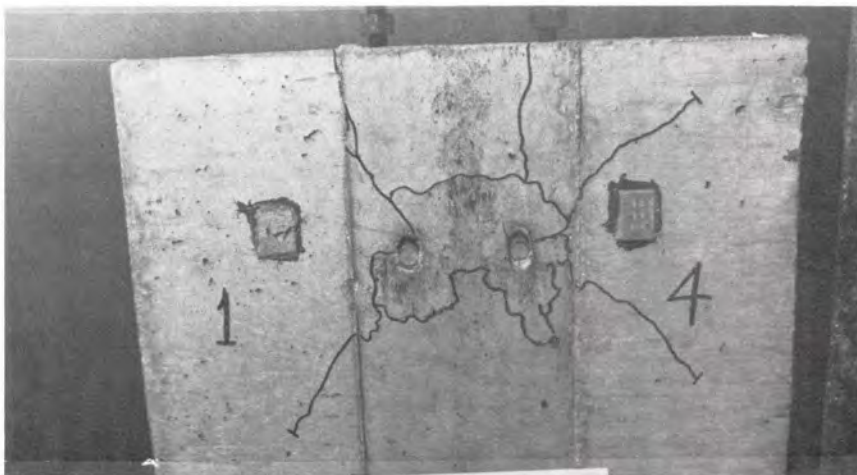
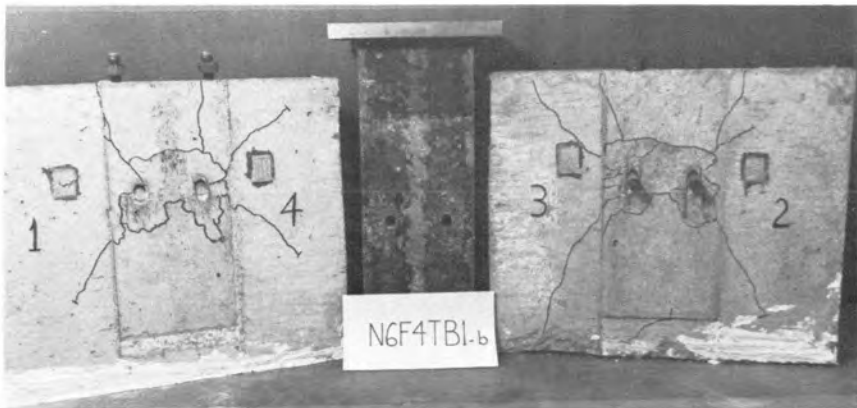


Figure 26 Companion Compression Pushout Failures

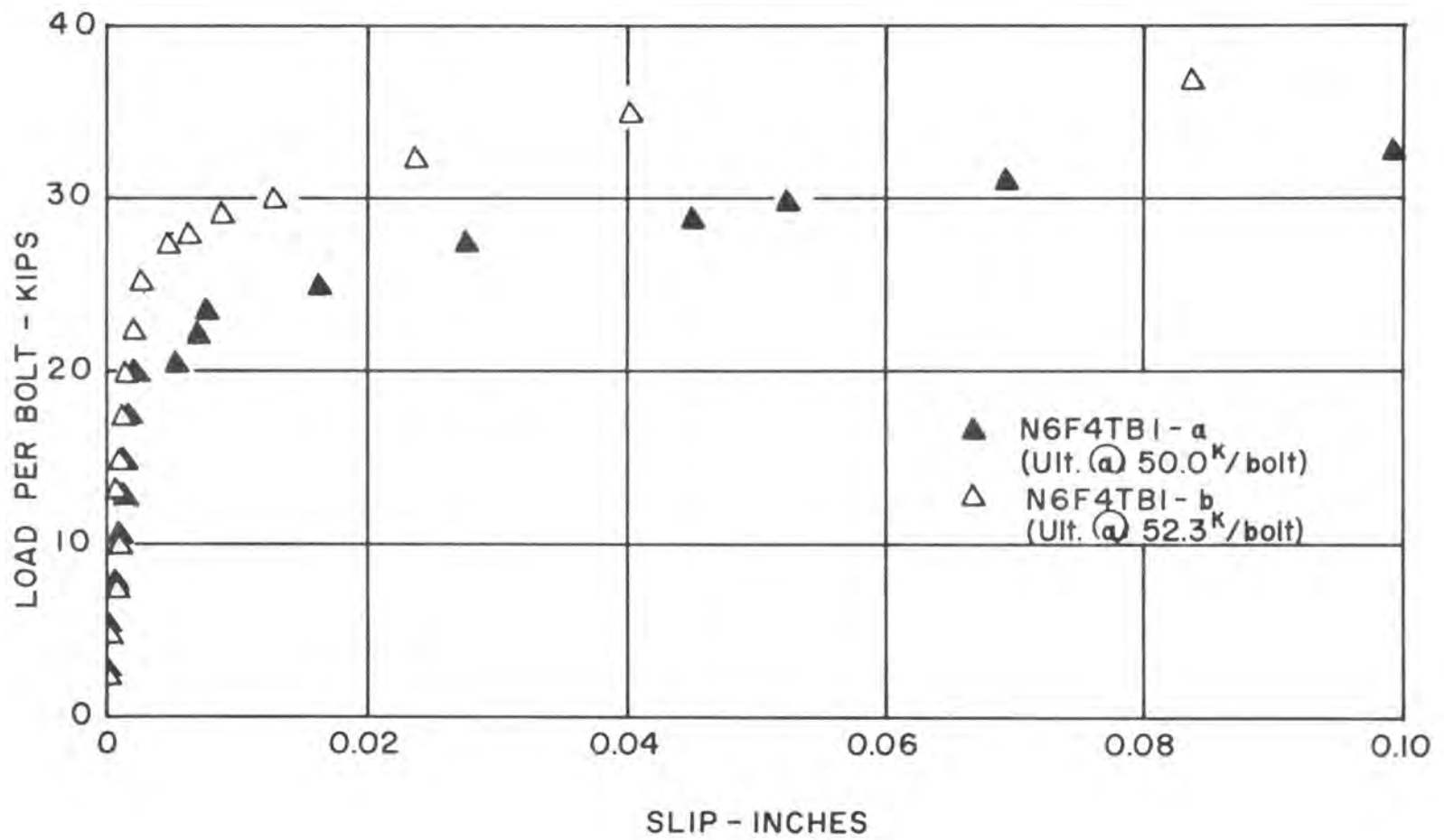


Figure 27 Load-Slip Comparison of Fatigue and Non-Fatigue Specimens

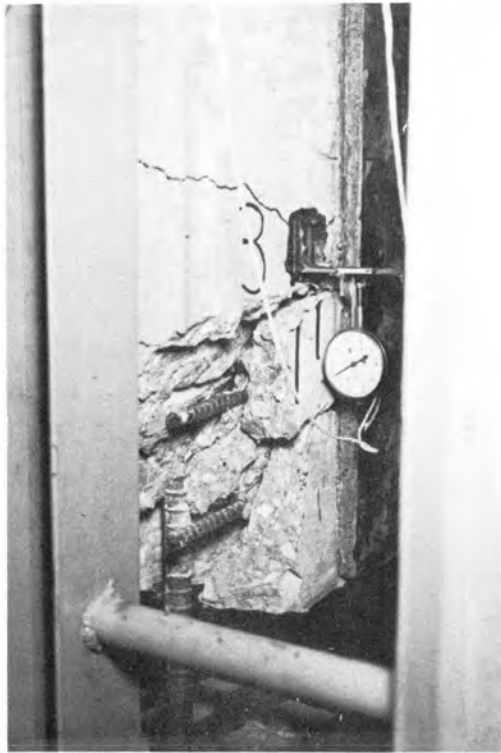


Figure 28a Cracking at
Connector -
Tension Failure

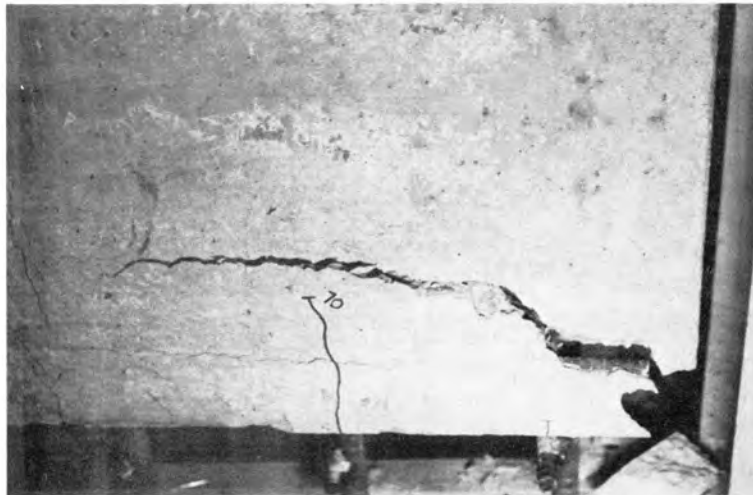


Figure 28b Splitting Slab - Tension Failure

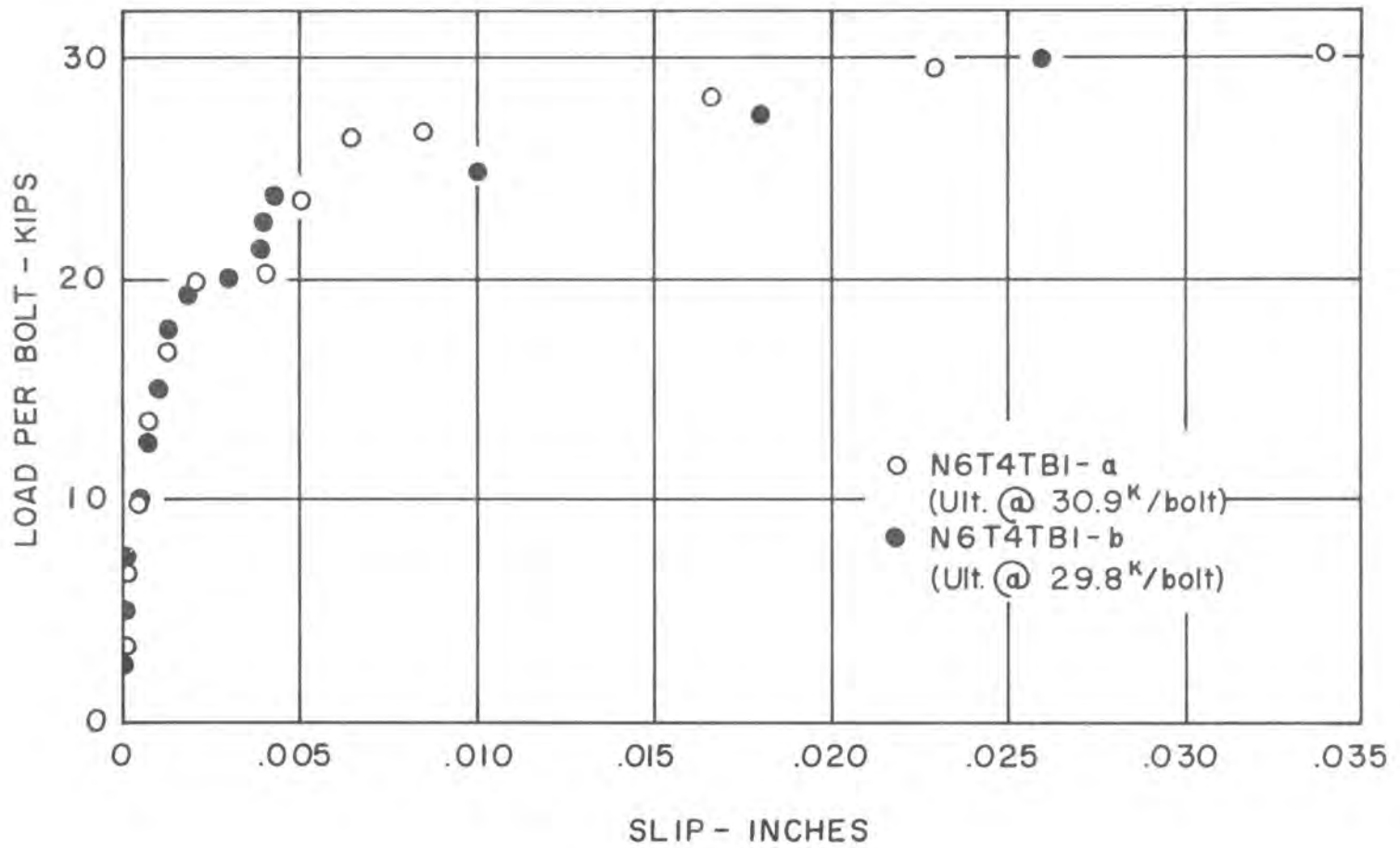


Figure 29 Load-Slip Tension Pushouts

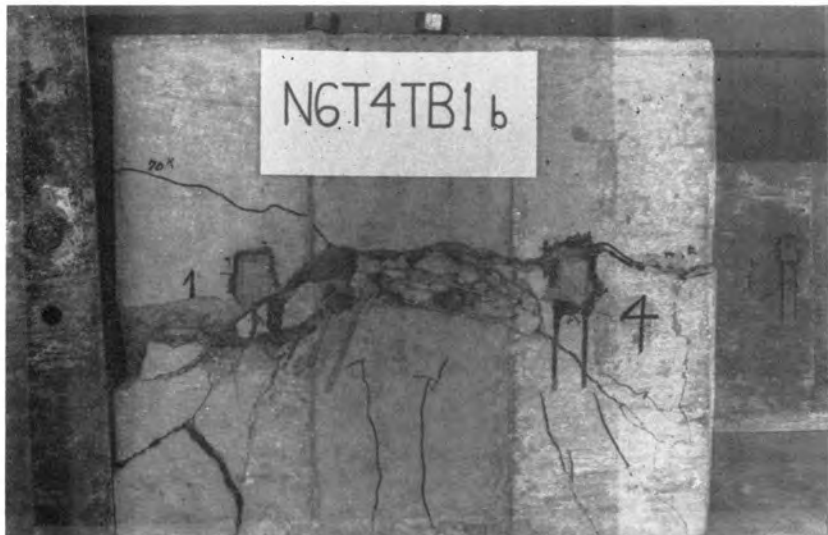


Figure 30 Typical Tension Failures

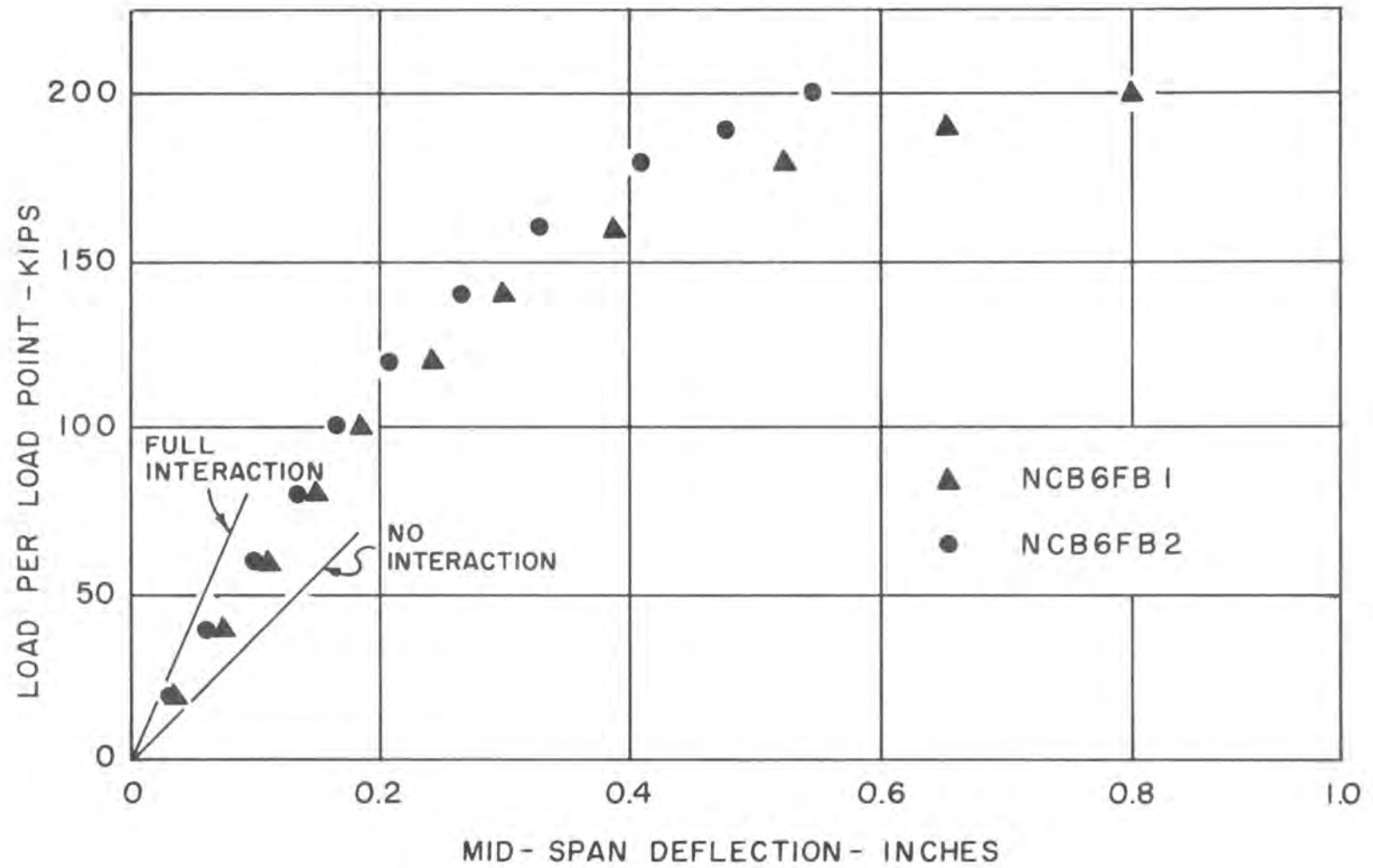


Figure 31 Deflection at Load Points

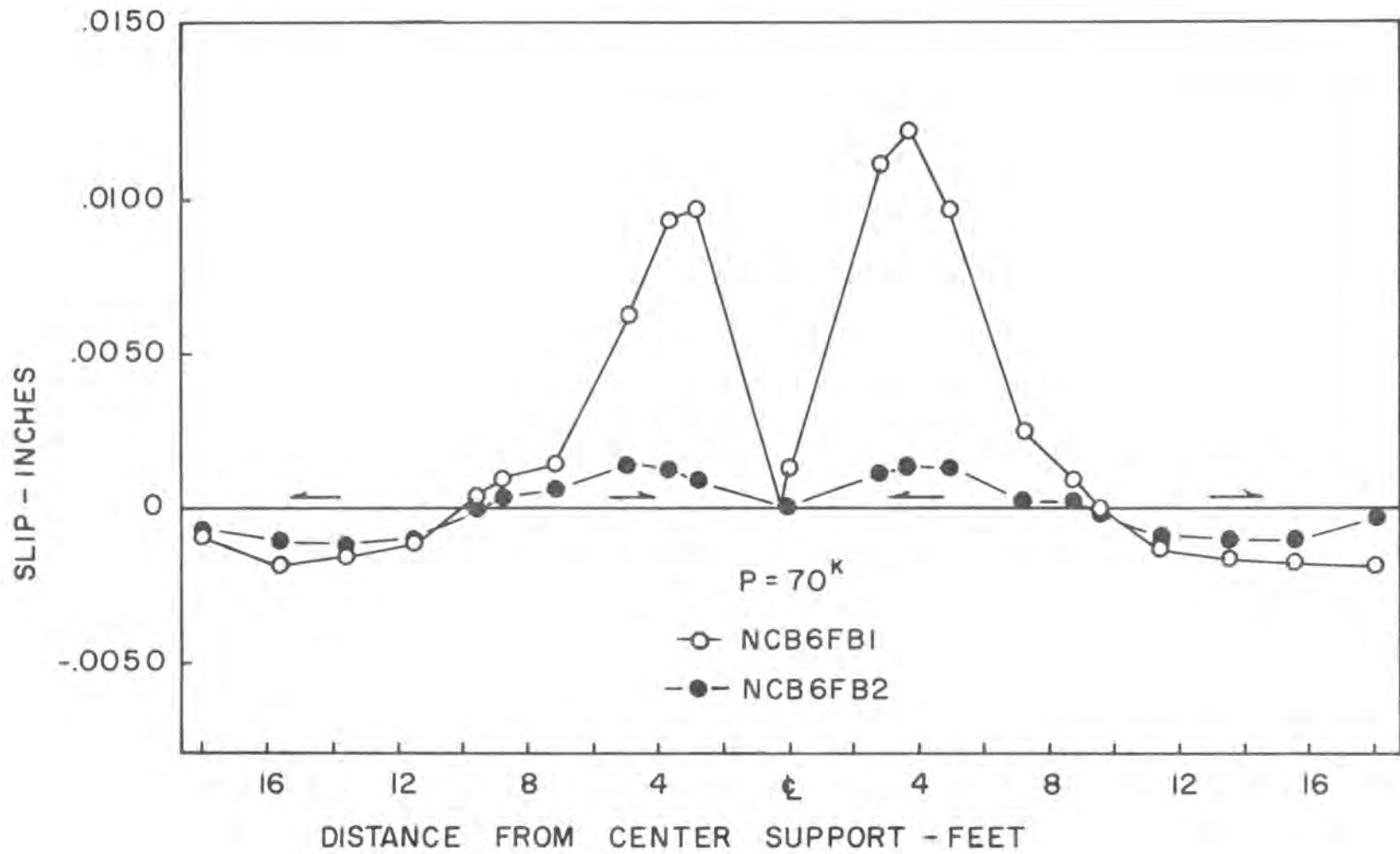


Figure 32 Slip Distribution at Working Load of NCB6FB1

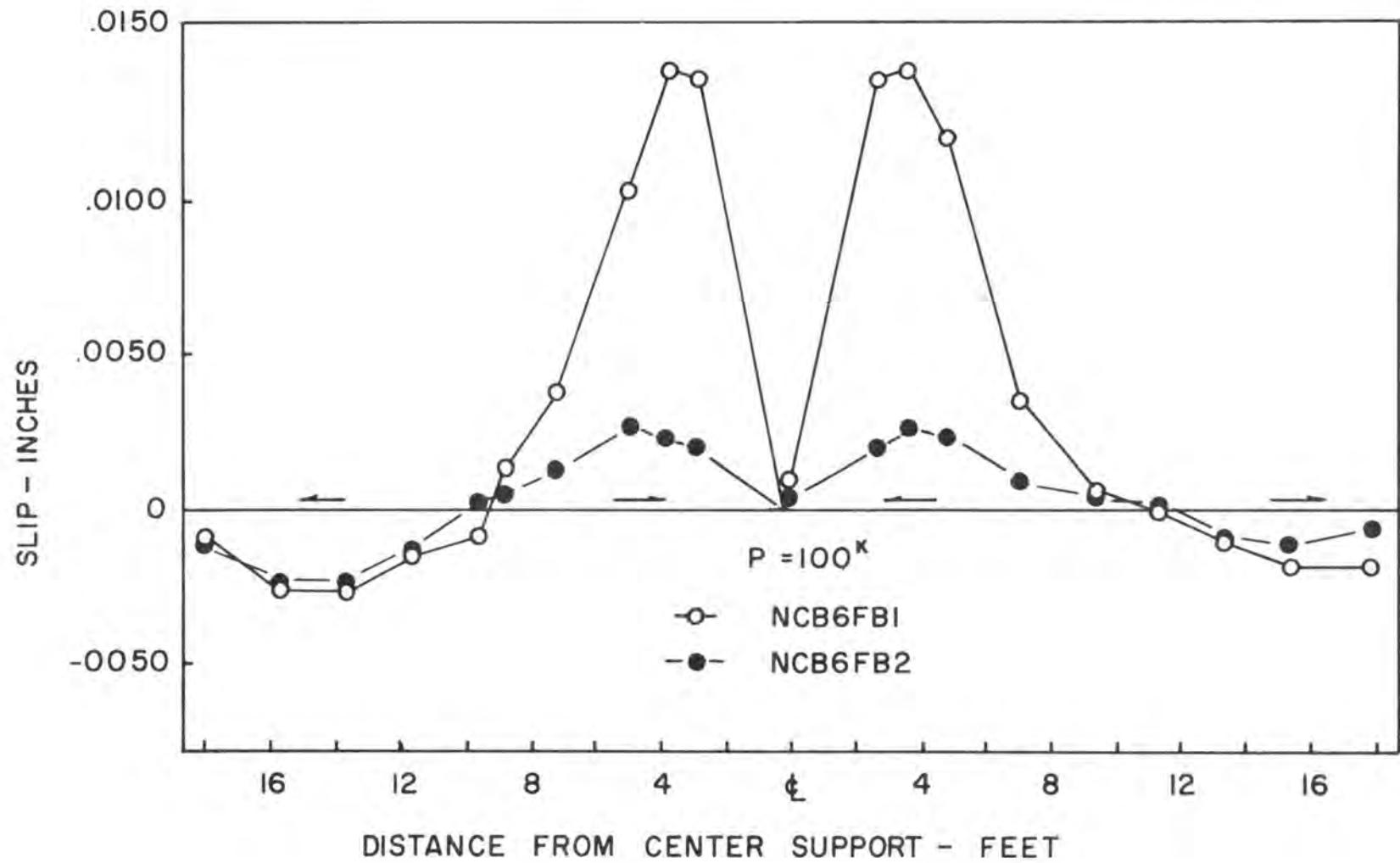


Figure 33 Slip Distribution at Working Load of NCB6FB2

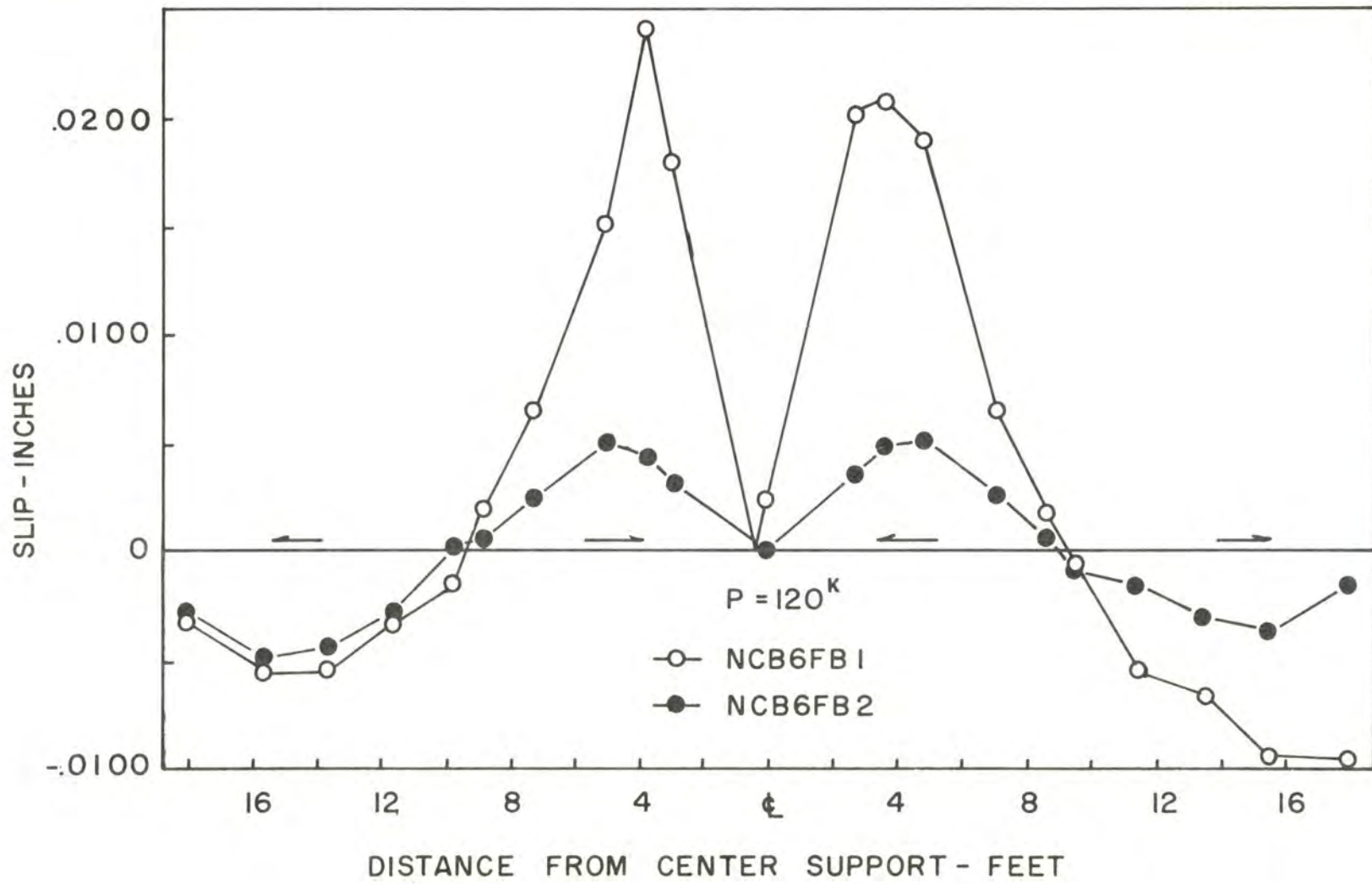


Figure 34 Slip Distribution at Yield Load of NCB6FB1

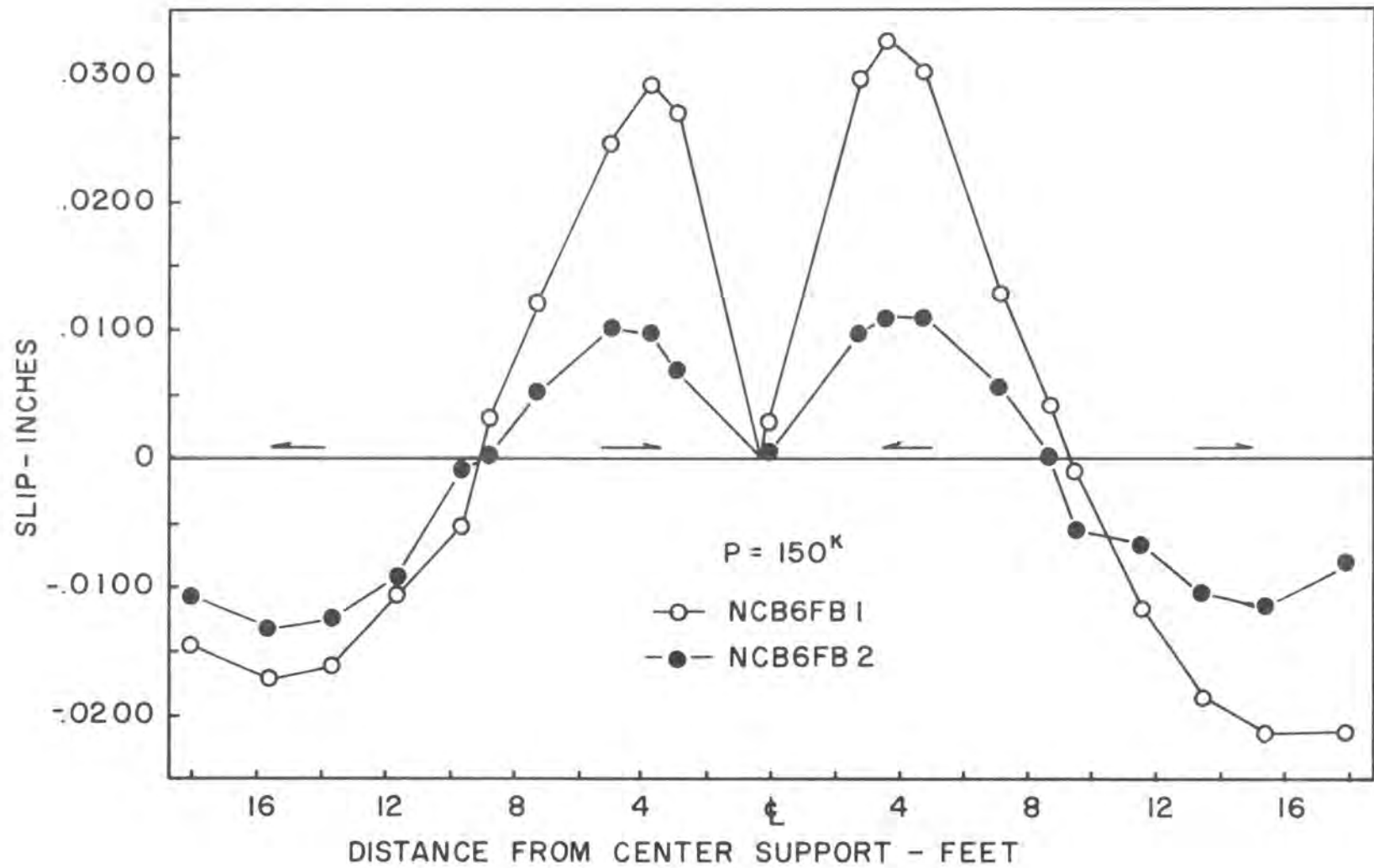


Figure 35 Slip Distribution at Yield Load of NCB6FB2

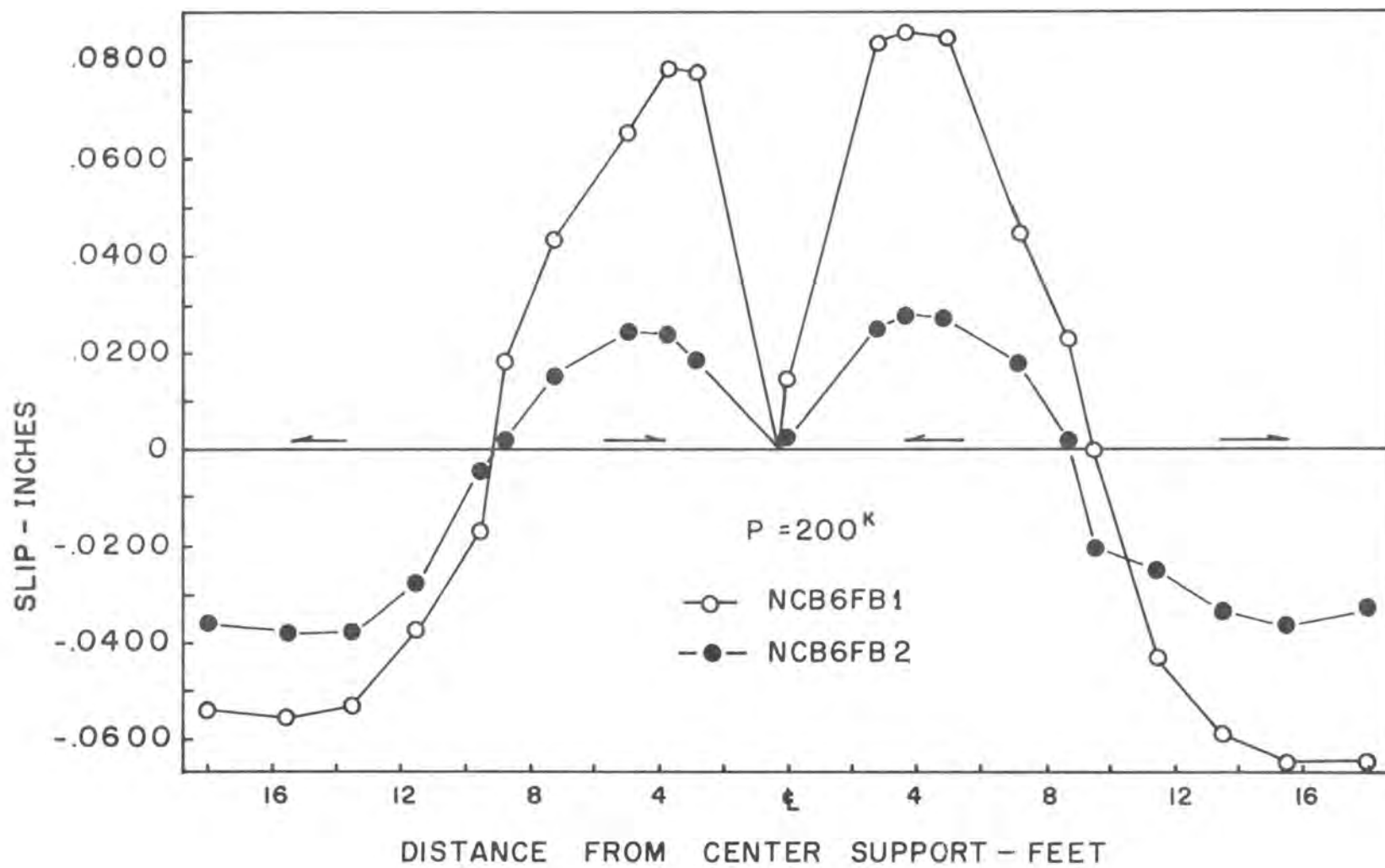


Figure 36 Slip Distribution at Final Load

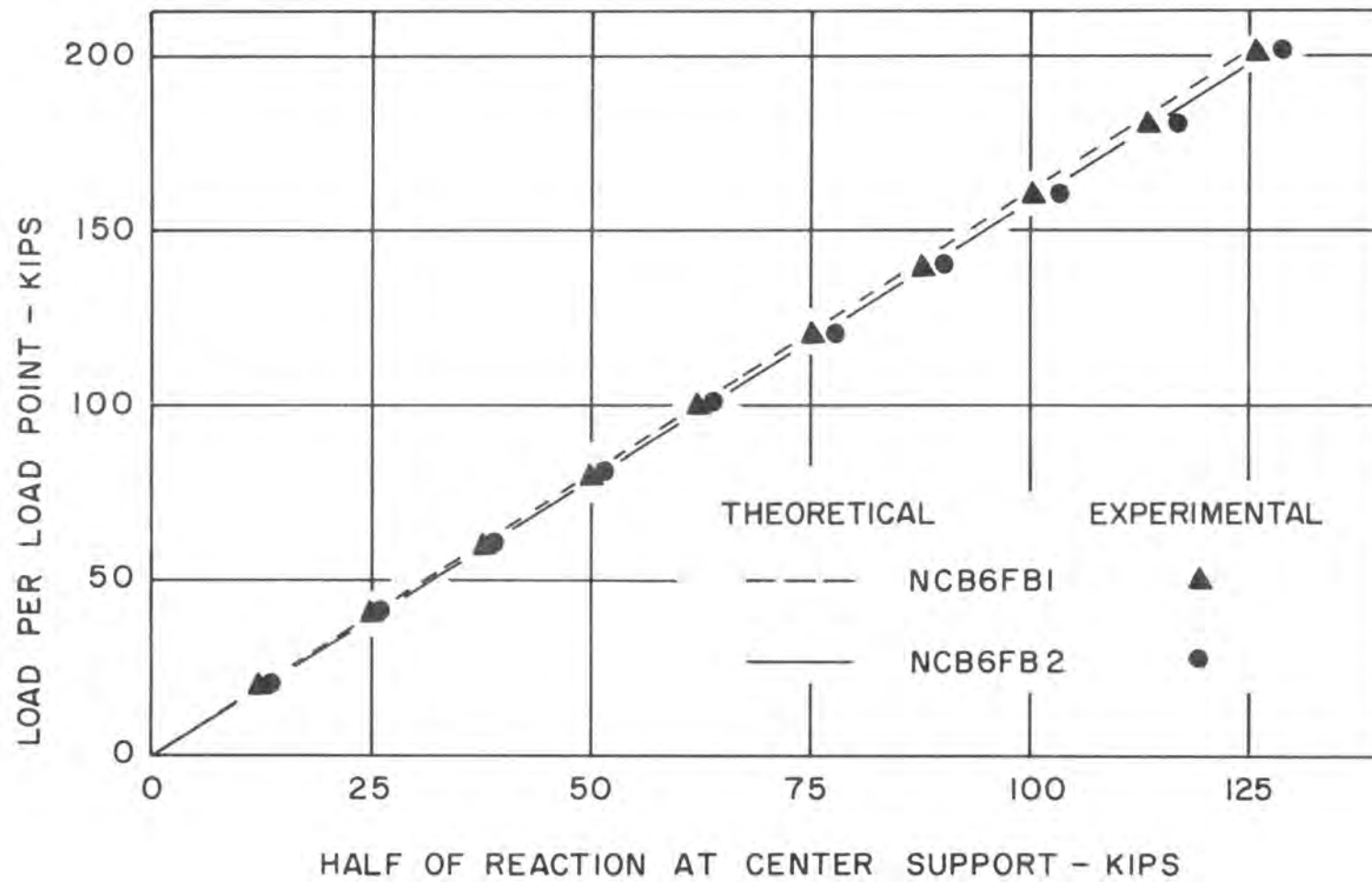


Figure 37 Applied Load vs Center Reaction

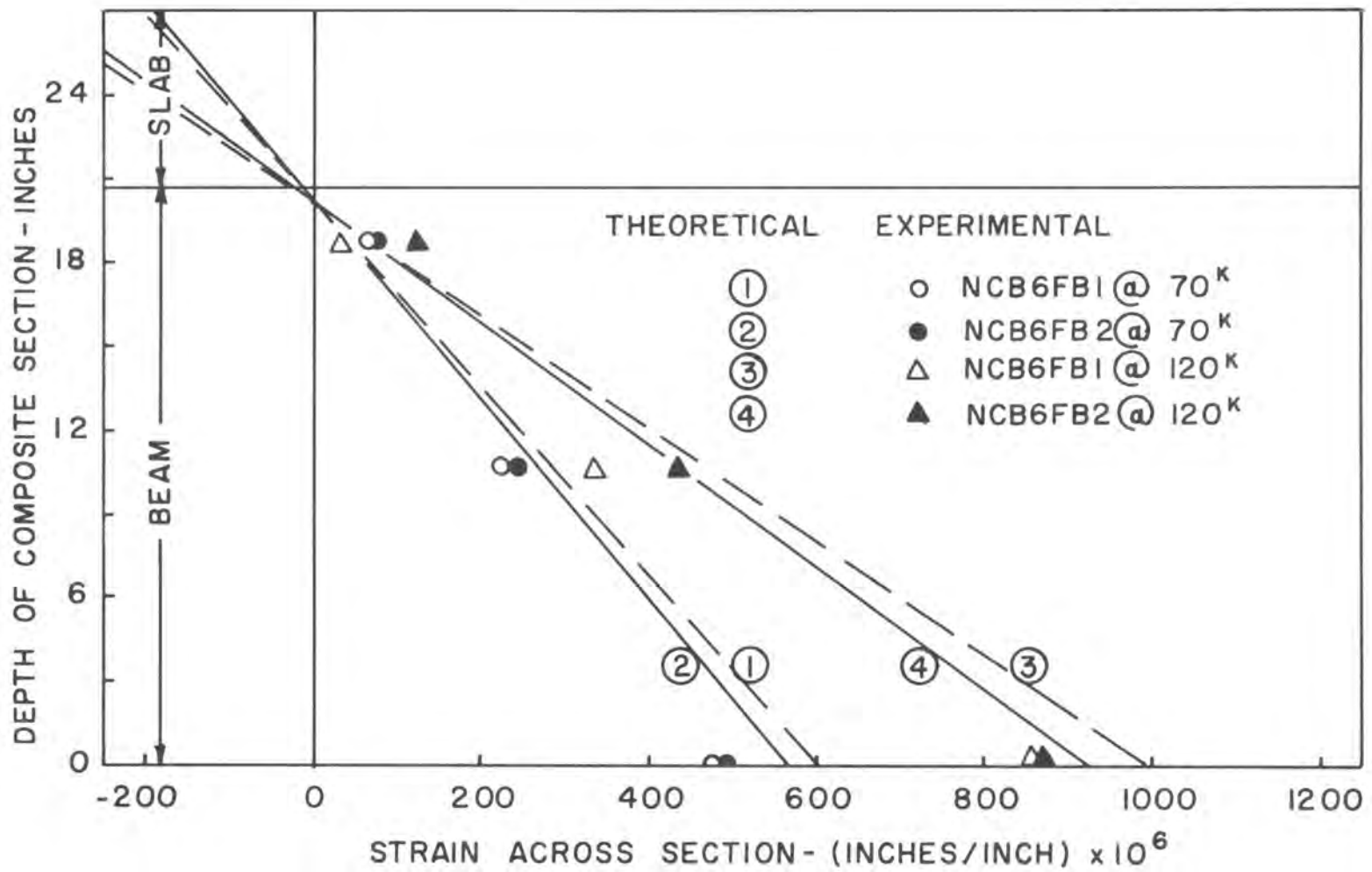


Figure 38 Working Strain Profile at Section A

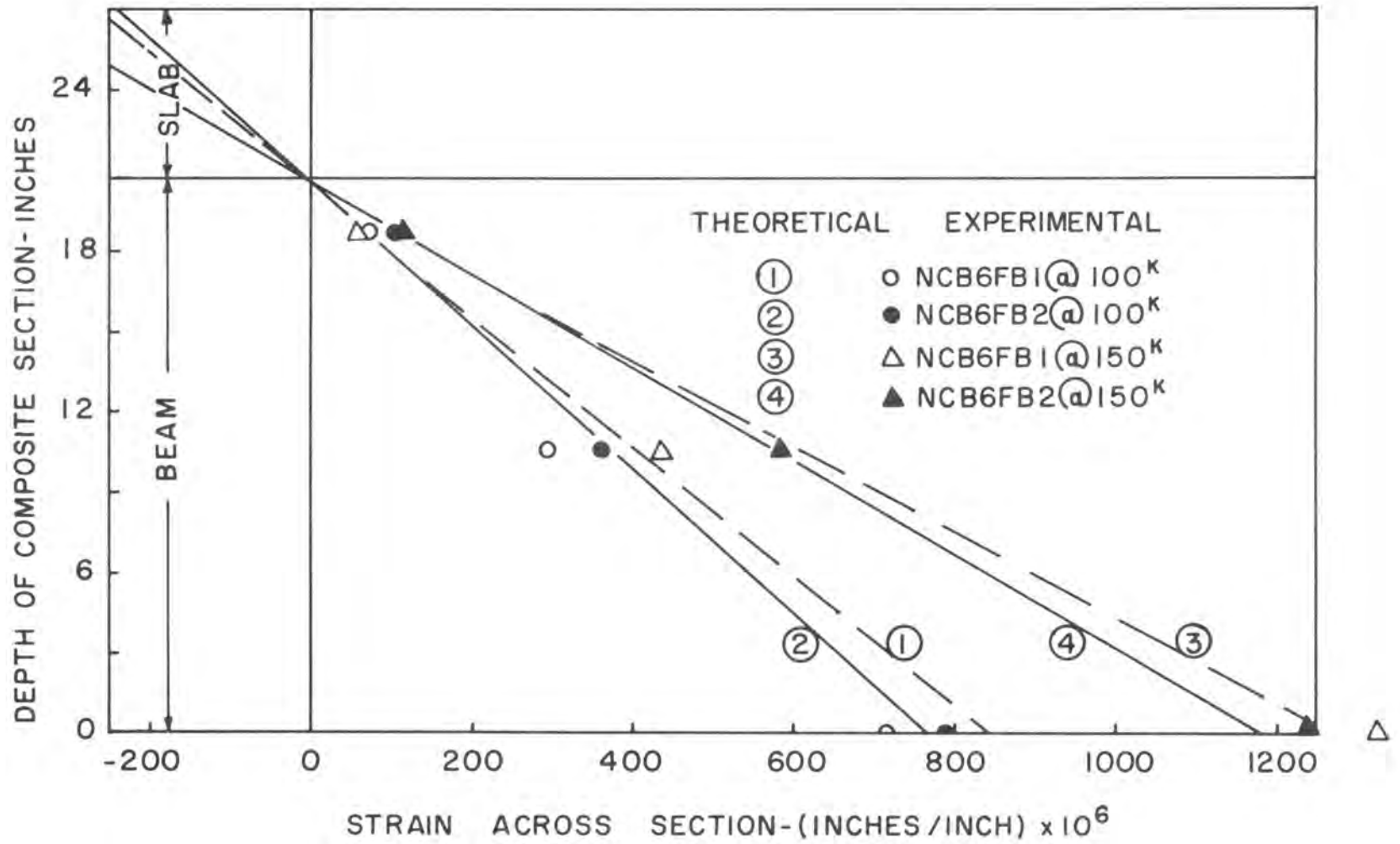


Figure 39 Yield Strain Profile at Section A

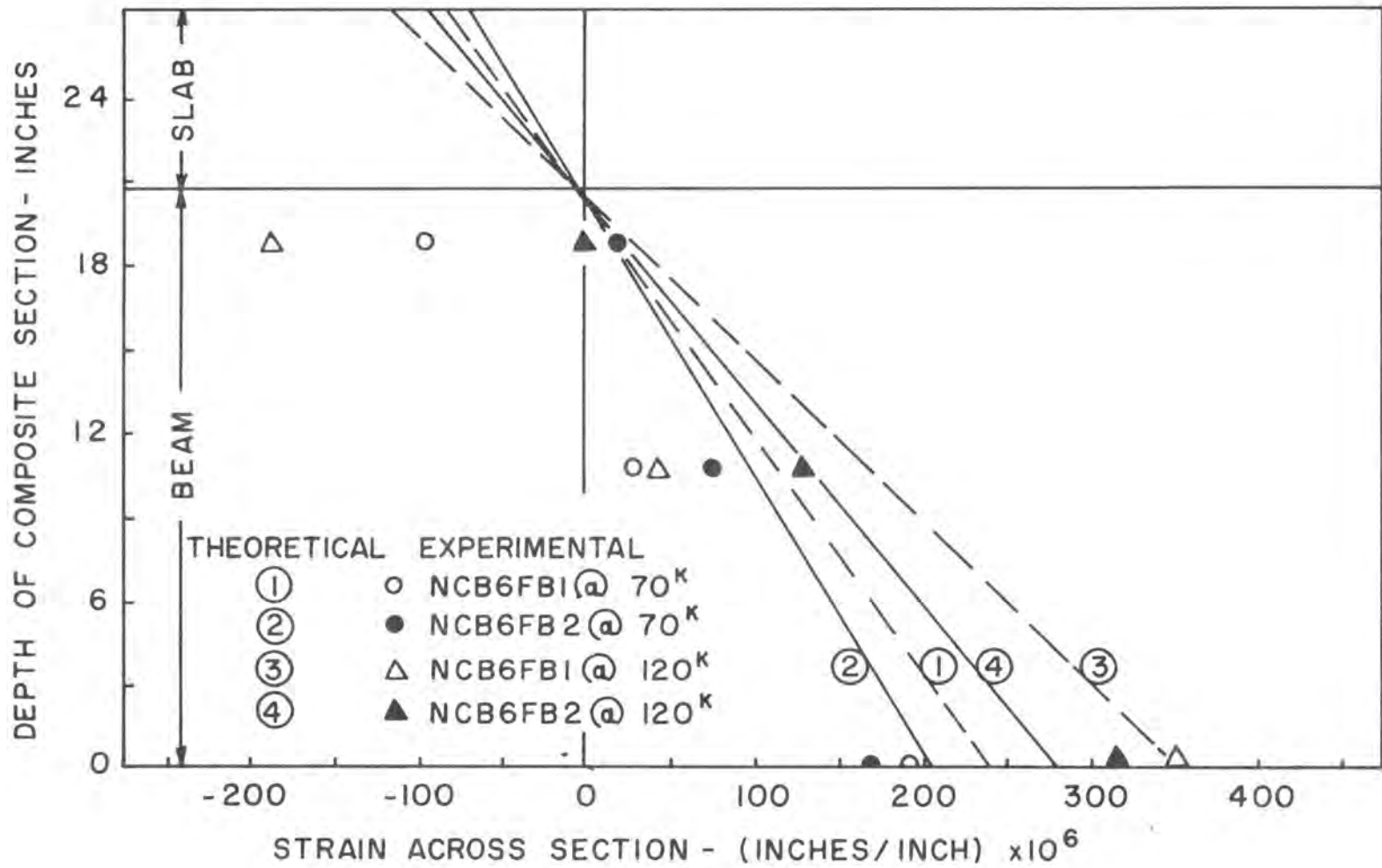


Figure 40 Working Strain Profile at Section B

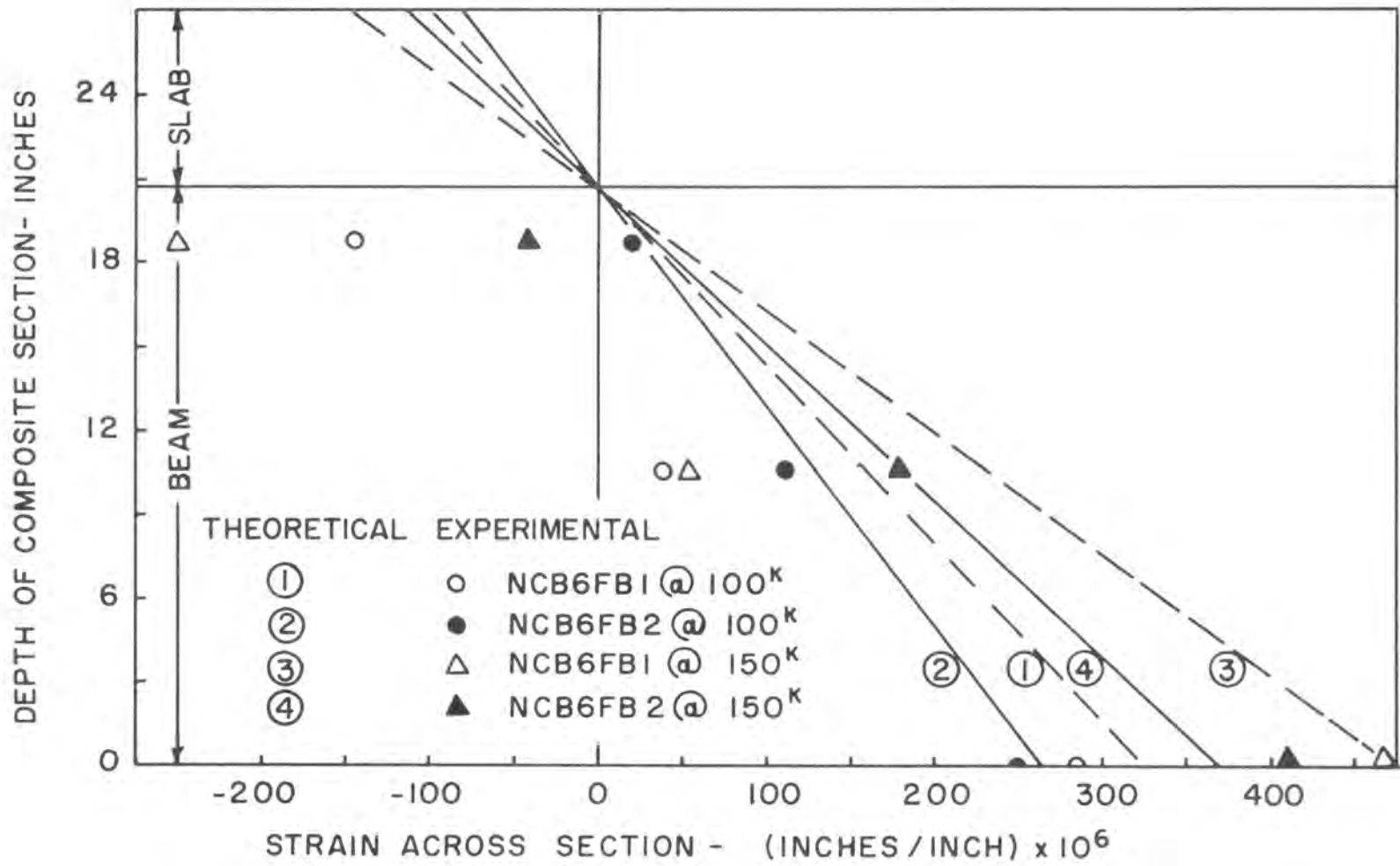


Figure 41 Yield Strain Profile at Section B

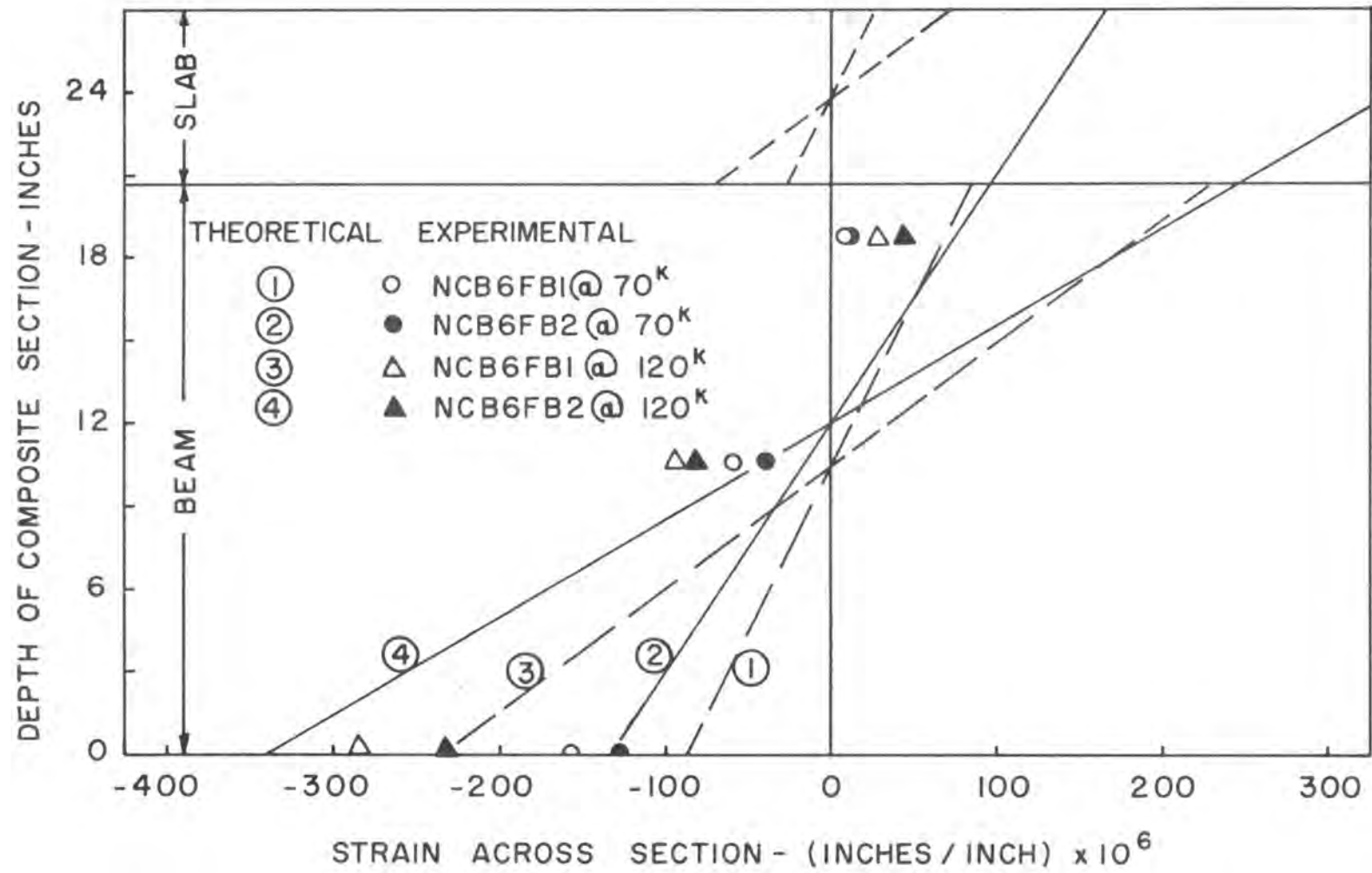


Figure 42 Working Strain Profile at Section C

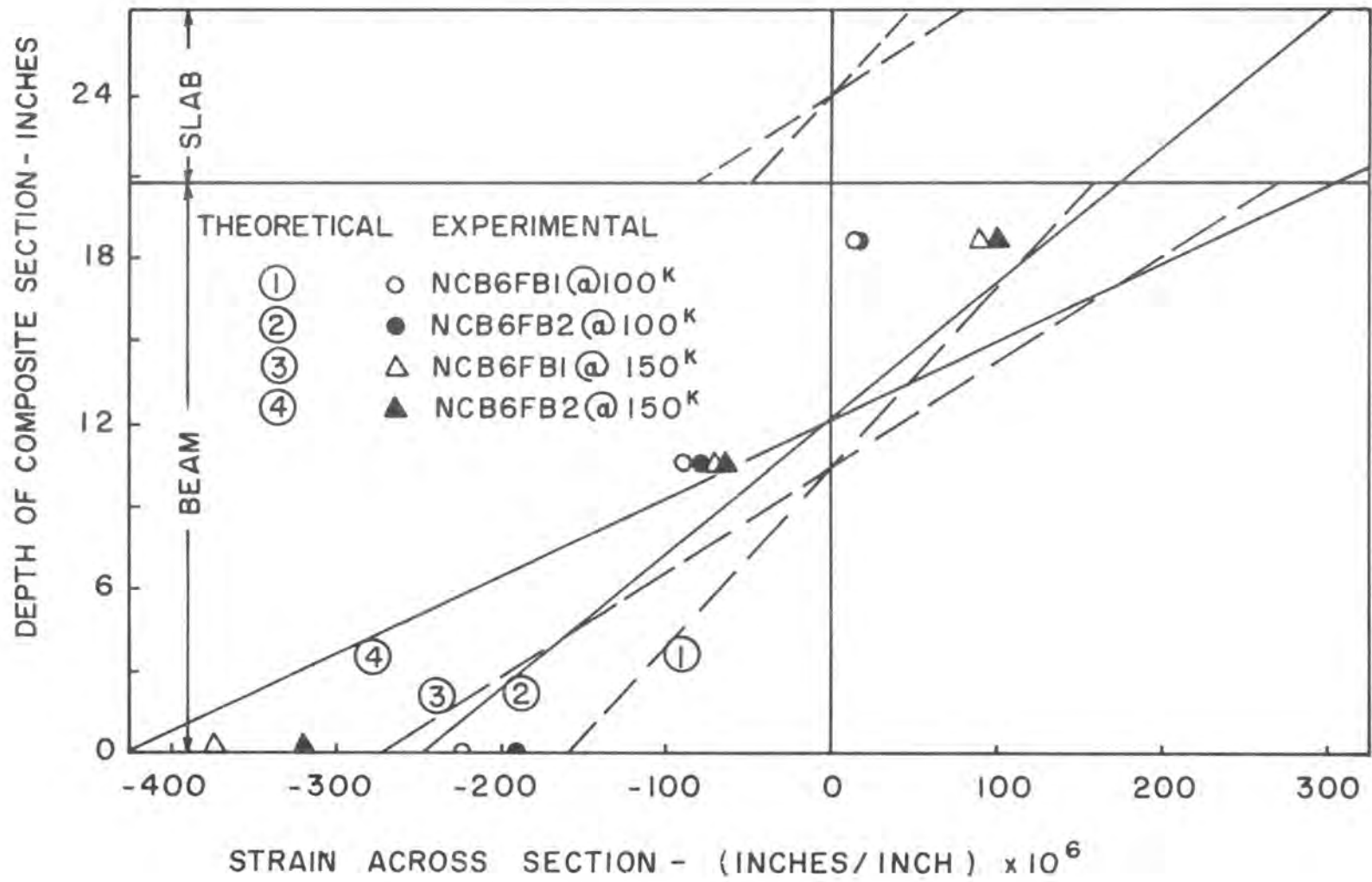


Figure 43 Yield Strain Profile at Section C

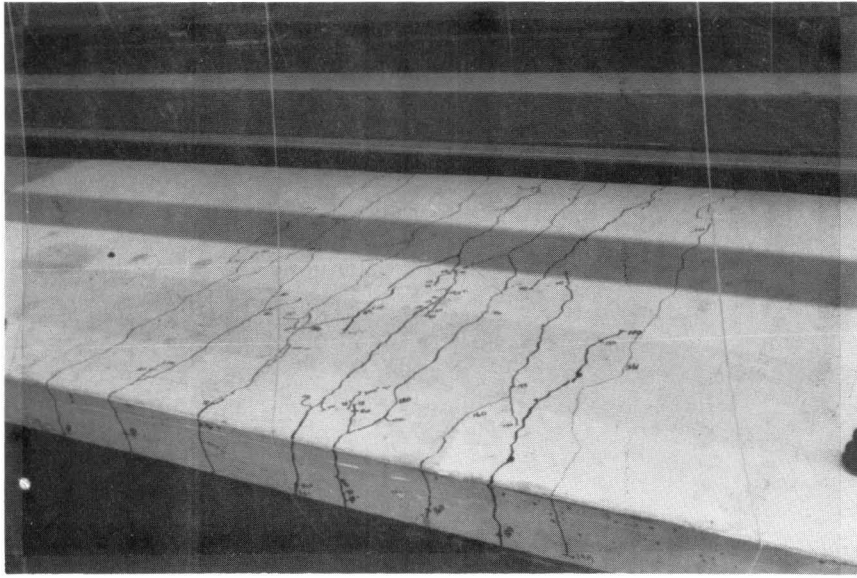


Figure 44 Negative Flexural Cracking Pattern - NCB6FB1

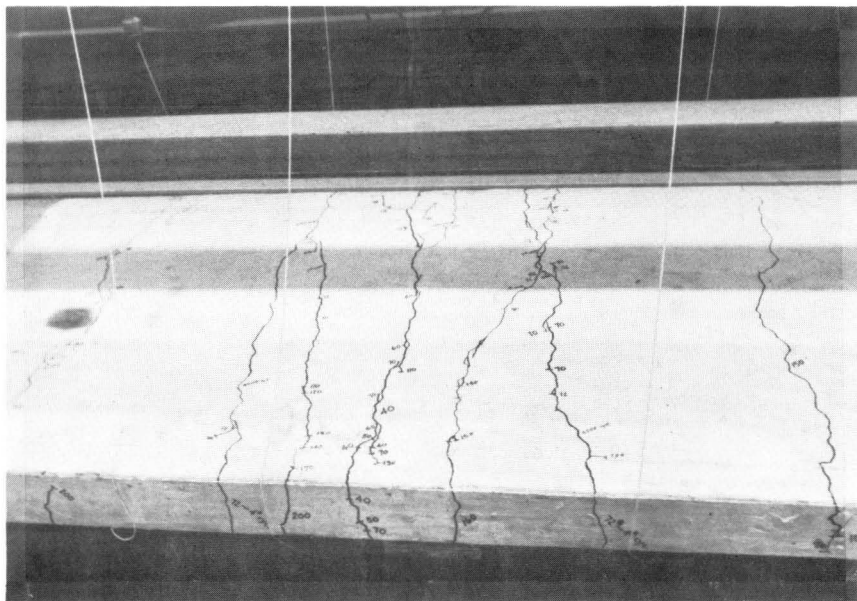


Figure 45 Negative Flexural Cracking Pattern - NCB6FB2

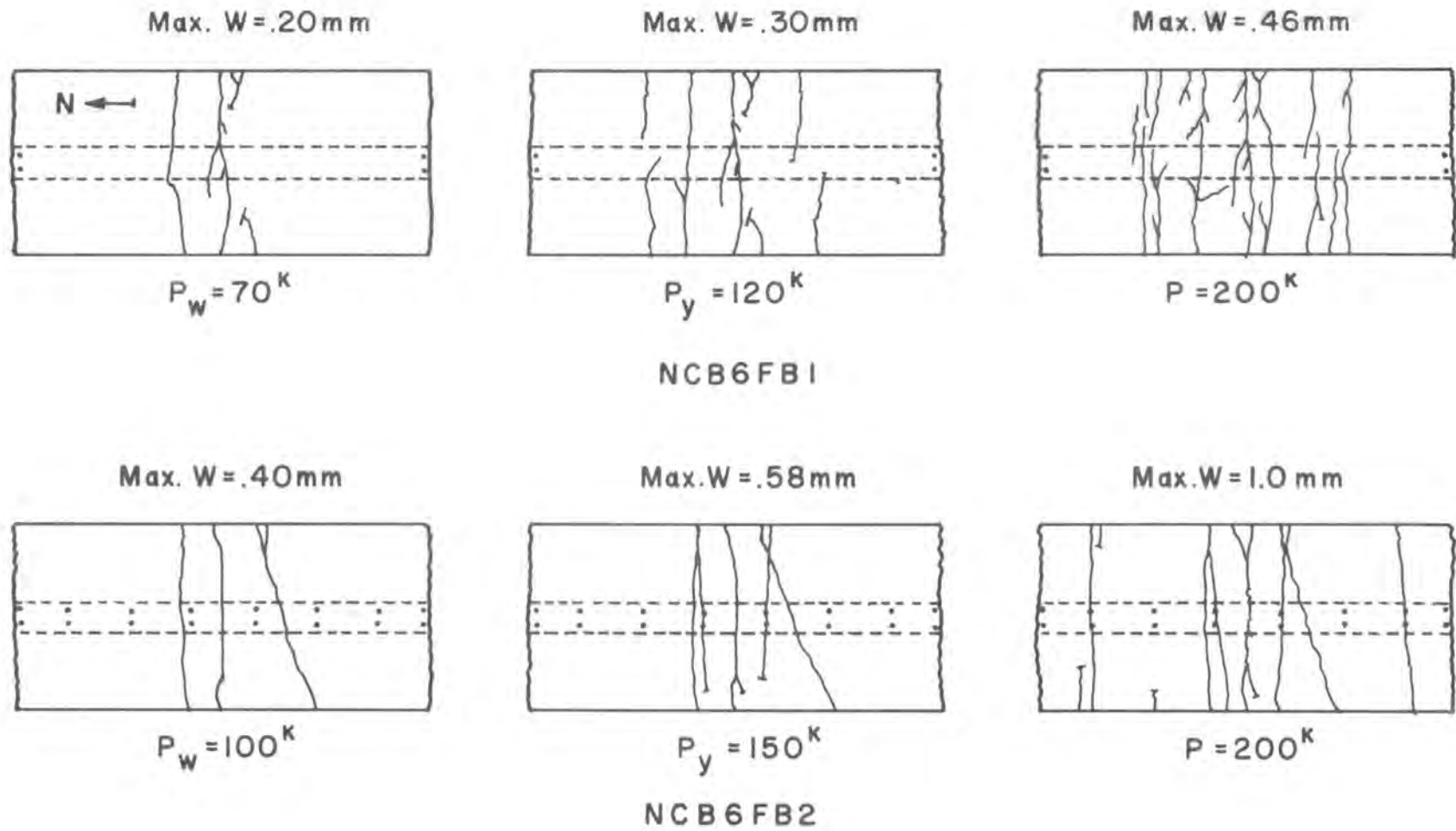


Figure 46 Comparative Cracking Patterns

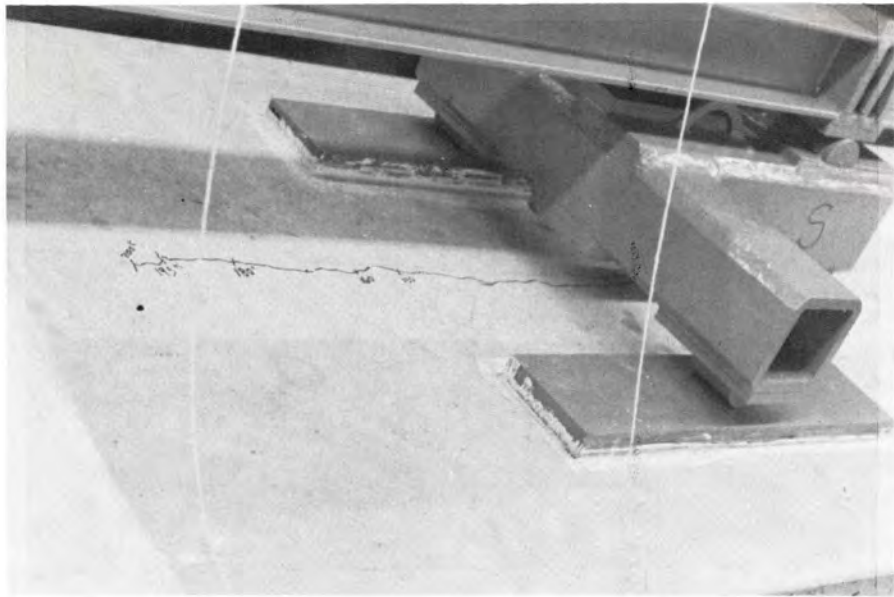


Figure 47 Longitudinal Cracking Pattern - NCB6FB1

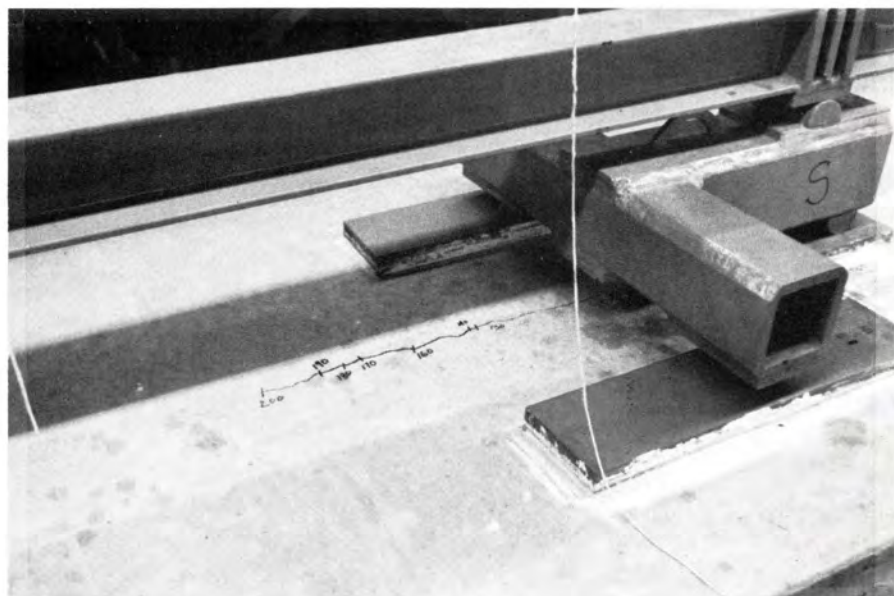


Figure 48 Longitudinal Cracking Pattern - NCB6FB2

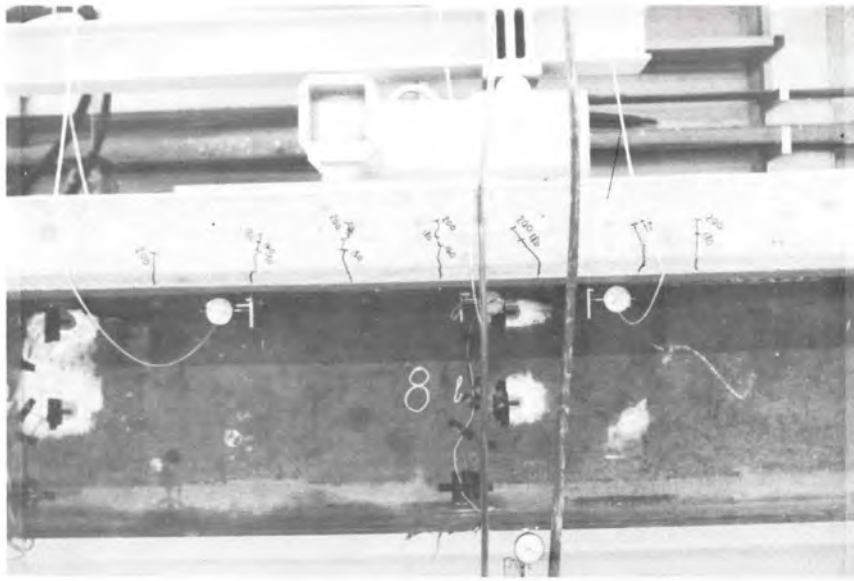


Figure 49 Positive Flexural Cracking Pattern - NCB6FB1

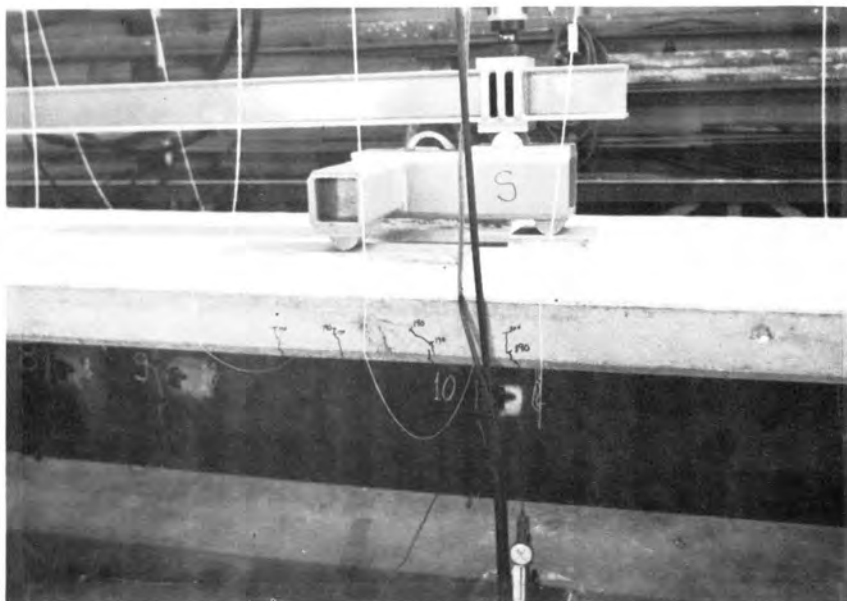


Figure 50 Positive Flexural Cracking Pattern - NCB6FB2

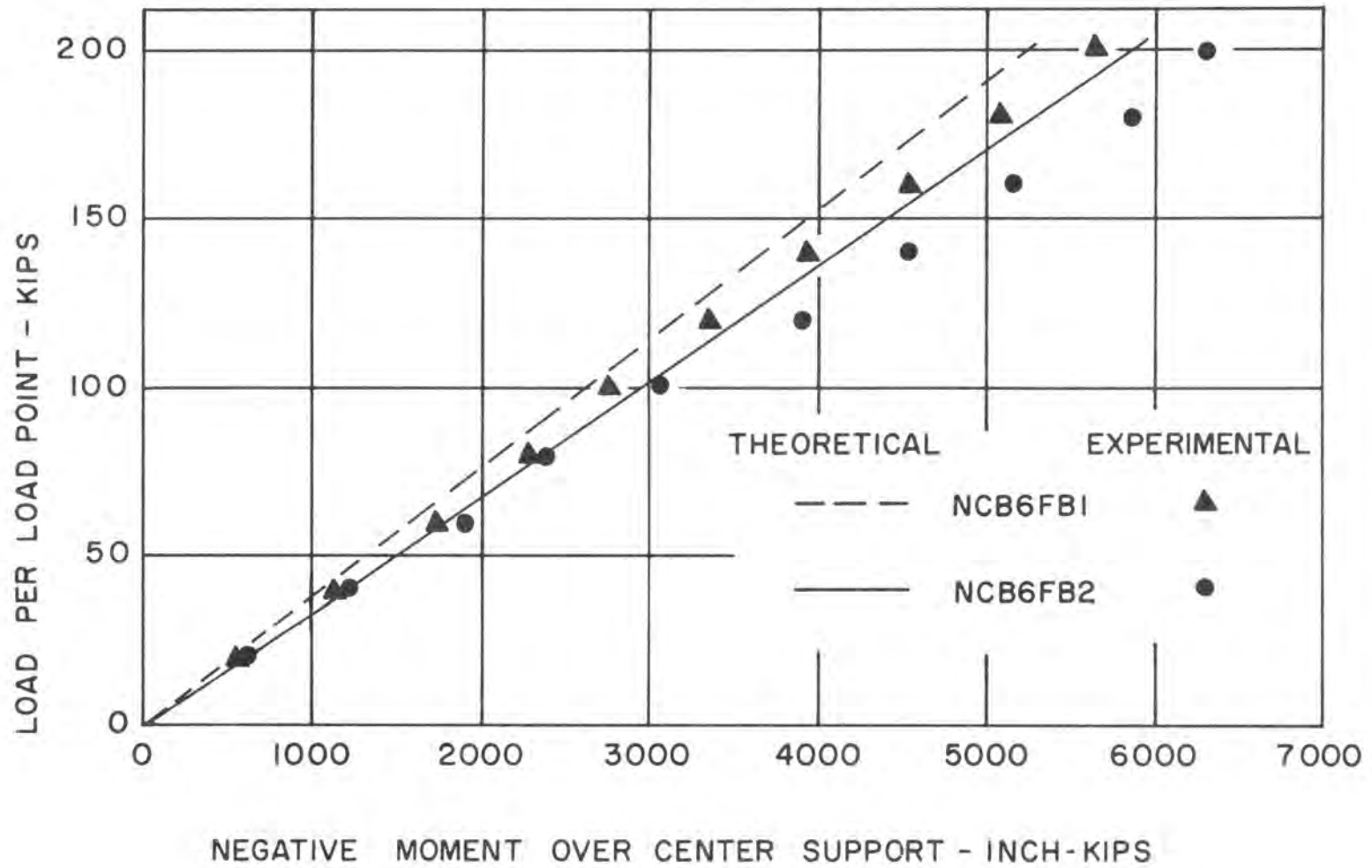


Figure 51 Applied Load vs Negative Moment

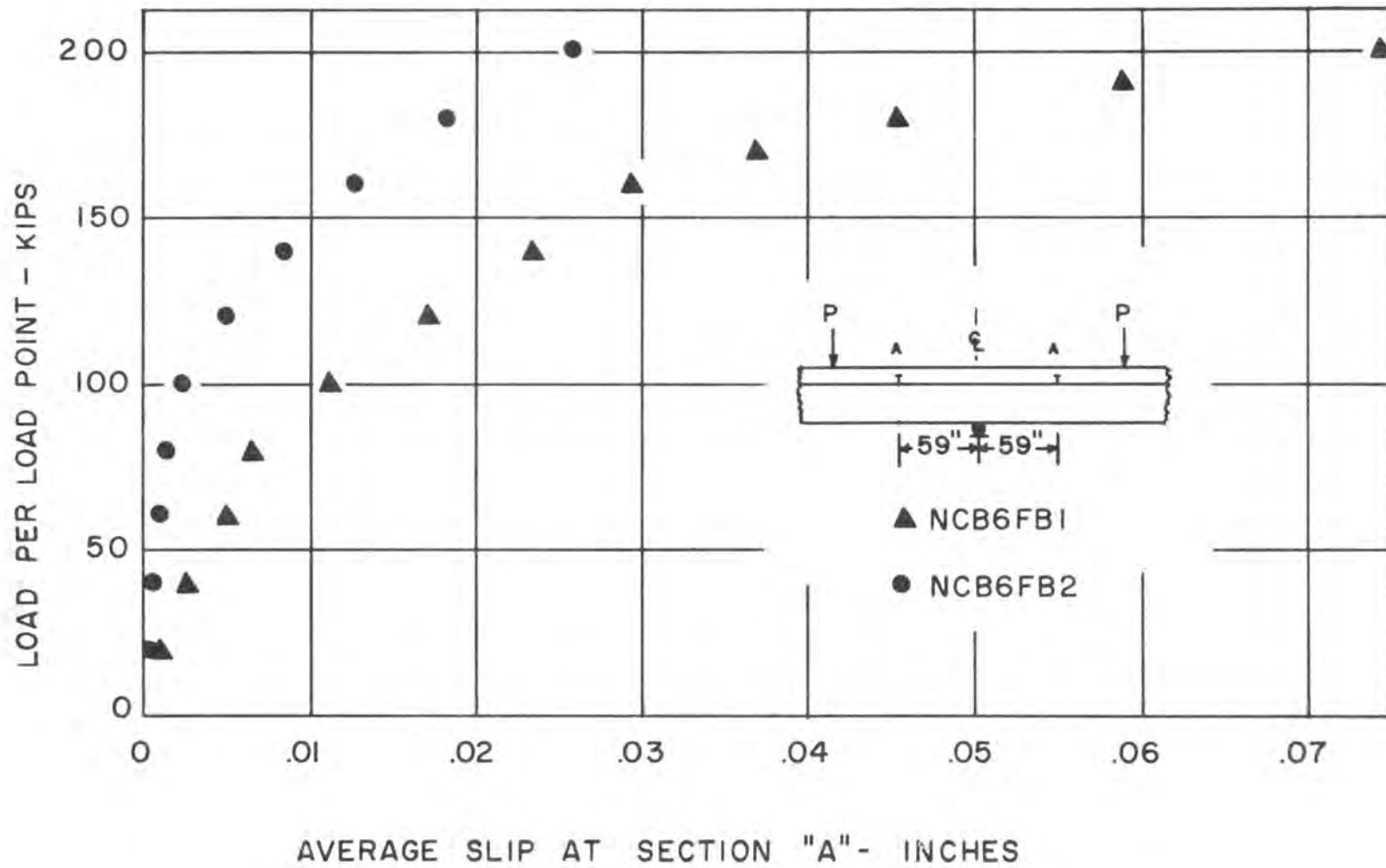


Figure 52 Load-Slip at a Typical Connector

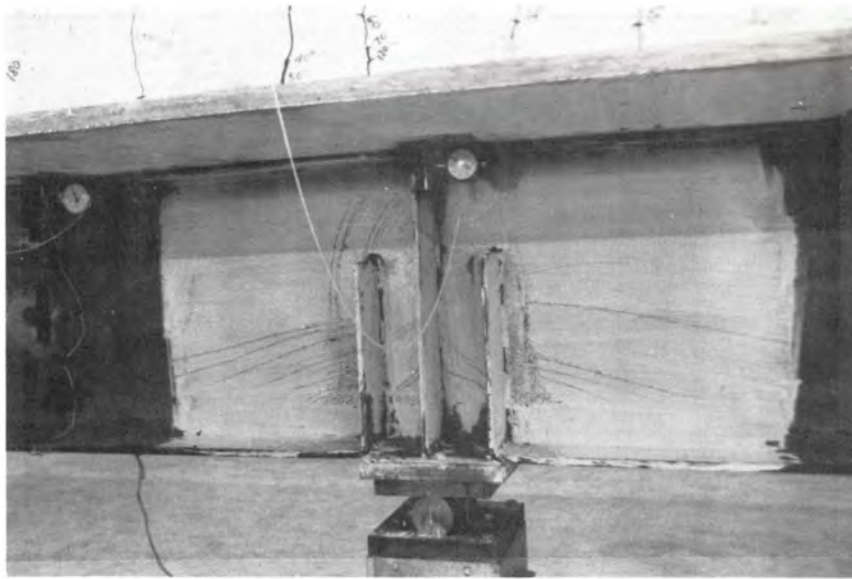


Figure 53 Yield Lines at Interior Support - NCB6FB1

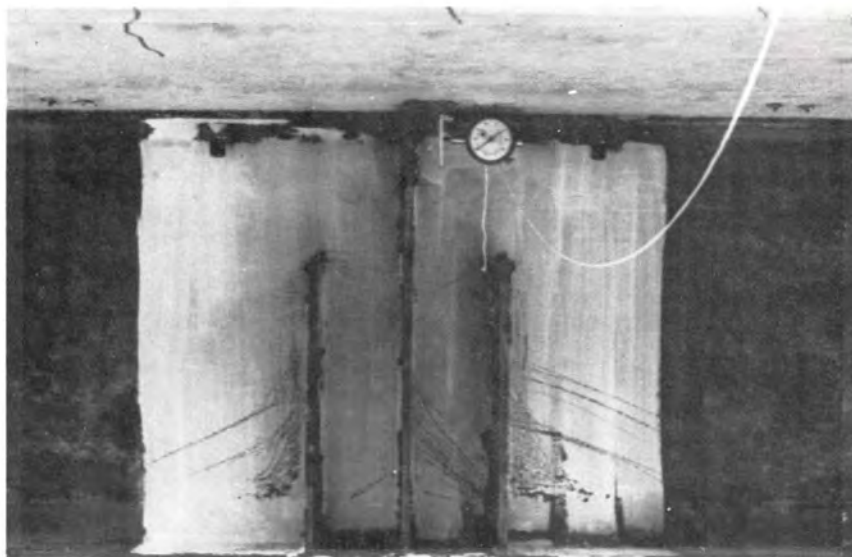


Figure 54 Yield Lines at Interior Support - NCB6FB2



Figure 55 Connectors
Intact
After Test

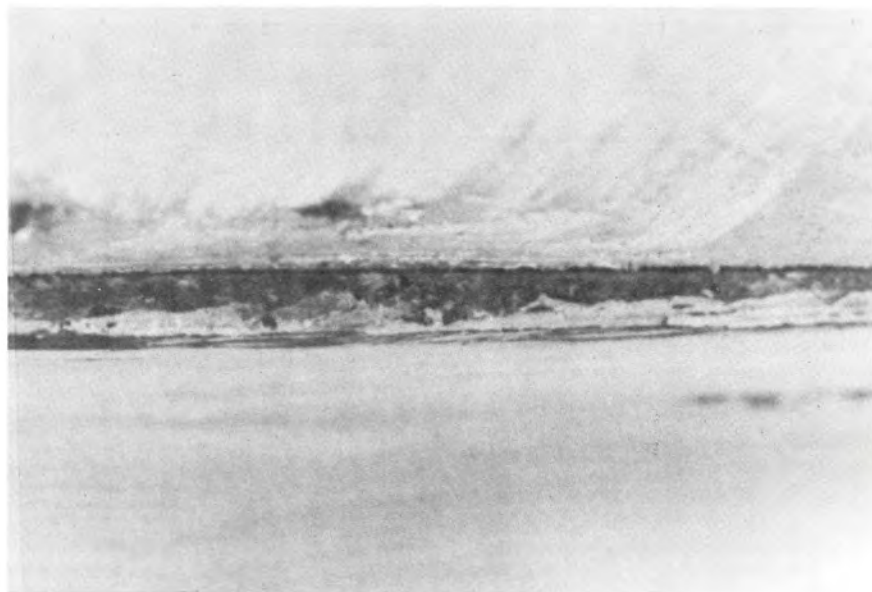
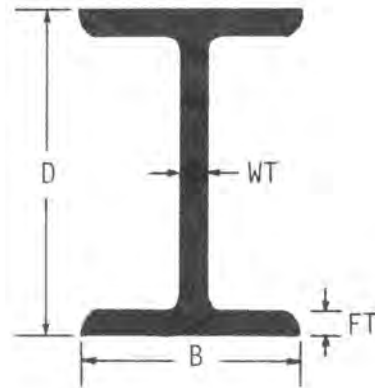


Figure 56 Separation During Test - NCB6FB1

TABLES

Table I

Actual Beam Dimensions



	A.I.S.C.	NCB6FB1	NCB6FB2
D	20.800	20.531	20.656
B	8.215	8.165	8.219
WT	0.375	0.395	0.399
FT	0.522	0.510	0.502
I	1140.700	1079.430	1090.050

All test beam measurements are average quantities.

Table II
Results of Non-Companion Pushouts

Specimen	f' _c psi	Load Range			Initial Static Loading		Fatigue Loading		Final Static Loading		Failure Type
		Min. Load K/Bolt	Max. Load K/Bolt	S* ksi	Yield Load K/Bolt	Resid. Slip Inches	# of Cycles x10 ⁶	Resid. Slip Inches	Yield Load K/Bolt	Ultim. Load K/Bolt	
N6F4TB1	4121	.885	5.30	10.0	--	.0001	5.00	.0014	8.75	32.50	Concrete
N6F4TB2	4436	.885	14.14	30.0	--	.0016	0.45	--	14.50	31.75	Concrete
N6F4TB3	4253	.885	14.14	30.0	--	.0036	10.00	.0233	--	--	None
		.885	18.58	40.0	--	--	0.70	.0088	--	--	None
		.885	25.00	54.6	--	--	0.12	--	--	--	Bolts
N6F4TB4	6690	4.425	17.68	30.0	17.5	.0032	10.00	.0189	18.00	32.62	Concrete
N6F4TB5	7061	.885	18.58	40.0	15.8	.0045	2.40	.0226	17.50	34.00	Concrete
N6F4TB6	6955	.885	22.98	50.0	23.0	.0098	0.20	.0077	--	--	Rammed
N6F4TB7	8217	.885	22.98	50.0	21.1	.0139	2.00	.0155	20.50	35.62	Concrete
N6F4TB8	8380	.885	15.30	32.6	--	.0005	2.00	.0008	19.25	34.25	Concrete
N6F4TB9	8310	.885	15.30	32.6	--	.0006	2.00	.0008	18.75	33.68	Concrete

* Range of stress per bolt

Table III

Results of Static Pushout Tests

Specimen	f'_c	Yield Load		Ultimate Load			Failure
		Average Slip	Load/Bolt	Average Slip	Load/Bolt	Resid. Slip	
N6F4TB1	4121	---	---	.1213 ^b	32.50	.0859	Concrete
N6F4TB2	4436	---	---	.1635 ^b	31.80	---	Concrete
N6F4TB3	4253	.0033	16.5 ^a	---	---	---	Bolts
N6F4TB4	6690	.0034	18.0 ^a	.1338 ^c	32.60	.0992	Concrete
N6F4TB5	7061	.0039	17.5 ^a	.1359 ^d	34.00	.0998	Concrete
N6F4TB6	6955	.0098	23.0	---	---	---	Rammed
N6F4TB7	8217	.0093	21.1	.0610 ^e	35.60	.0569	Concrete
N6F4TB8	8380	.0040	20.5 ^a	.0838 ^f	34.20	---	Concrete
N6F4TB9	8310	.0032	19.5 ^a	.1782 ^g	33.70	.1396	Concrete
N6F4TB1a	7026	.0053	20.6 ^a	.1805 ^e	50.00	---	Bolts
N6F4TB1b	7522	.0061	28.4	.0405 ^e	52.25	---	Bolts

^aDetermined after fatigue loading^b30.0 k/bolt^d32.5 k/bolt^f34.25 k/bolt^c31.5 k/bolt^e35.0 k/bolt^g33.75 k/bolt

Table IV
Results of Companion Compression Pushouts

Specimen	f' _c psi	Load Range			Initial Static Loading		Fatigue Loading		Final Static Loading		Failure Type
		Min. Load K/Bolt	Max. Load K/Bolt	S* ksi	Yield Load K/Bolt	Resid. Slip Inches	# of Cycles x10 ⁶	Resid. Slip Inches	Yield Load K/Bolt	Ultim. Load K/Bolt	
N6F4TB1a	7026	.885	15.30	32.6	--	.0006	2.0	.0012	20.60	50.00	Bolts
N6F4TB1b	7522	--	--	--	--	--	--	--	28.40	52.25	Bolts

* range of stress per bolt

Table V
Results of Companion Tension Pushouts

Specimen	f' _c psi	Yield Load K/Bolt	Yield Slip Inches	Ultimate Load K/Bolt	Maximum* Slip Inches	Failure Type
N6T4TB1a	6700	22.60	.00177	30.90	.0342	Concrete
N6T4TB1b	7168	22.25	.00101	31.50	.0263	Concrete

* measurable (at approximately 80% of ultimate)

Table VI
Results of Cylinder Tests

Specimen	Compressive Strength psi	Modulus of Elasticity psi $\times 10^6$
N6F4TB1	4121 \pm 68*	3.80 \pm .02*
N6F4TB2	4436 \pm 67	3.96 \pm .00
N6F4TB3	4253 \pm 102	4.03 \pm .02
N6F4TB4	6690 \pm 38	4.31 \pm .08
N6F4TB5	7061 \pm 44	4.39 \pm .00
N6F4TB6	6955 \pm 176	4.15 \pm .02
N6F4TB7	8217 \pm 68	4.52 \pm .05
N6F4TB8	8380 \pm 156	4.50 \pm .01
N6F4TB9	8310 \pm 160	4.35 \pm .08
NCB6FB1	7338 \pm 157	4.37 \pm .08
N6F4TB1a	7026 \pm 82	3.98 \pm .10
N6F4TB1b	7522 \pm 91	4.51 \pm .03
NCB6FB2	7654 \pm 58	5.42 \pm .23
N6T4TB1a	6700 \pm 190	5.17 \pm .07
N6T4TB1b	7168 \pm 36	5.21 \pm .02

* standard deviation

Table VII
 Coupon Results
 Yield Strength-ksi

Specimen	Top Flange	Web	Bottom Flange	Average
NCB6FB1	35.37 ± .57*	39.35 ± .62	34.53 ± .21	37.09
NCB6FB2	35.78 ± .61	38.31 ± .63	36.35 ± .43	37.14

Table VIII
 Coupon Results
 Static Yield Strength-ksi

Specimen	Top Flange	Web	Bottom Flange	Average
NCB6FB1	34.05 ± .34	38.14 ± .70	33.23 ± .22	35.83
NCB6FB2	34.28 ± .46	36.34 ± .73	34.35 ± .66	35.28

Table IX
 Coupon Results
 Modulus of Elasticity- $\text{psix}10^6$

Specimen	Top Flange	Web	Bottom Flange	Average
NCB6FB1	27.42 ± .31	28.72 ± .15	29.07 ± .40	28.47
NCB6FB2	29.41 ± .03	30.25 ± .17	29.81 ± .20	29.92

Table X
 Reinforcing Bar Specimen Results
 High-Strength Steel

Specimen	Yield Strength-ksi	Modulus of Elasticity $\text{psix}10^6$
#4	68.2 ± .03	29.2 ± .09
#5	67.5 ± .12	27.5 ± .17
#7	59.0 ± .52	28.4 ± .39

* standard deviation

Table XI

Analyses Results

Test Beams

NCB6FB1

	Theoretical	Experimental
Working Load	75.8	70.0
Yielding Load	137.9	119.2
Ultimate Load [*]	161.7	---

NCB6FB2

	Theoretical	Experimental
Working Load	78.6	100.4
Yielding Load	151.4	153.3
Ultimate Load [*]	209.2	---

* Load at which plastic hinge over center support forms

BIBLIOGRAPHY

1. Wang, C. K., and Salmon, C. G., Reinforced Concrete Design, International Textbook Company, Scranton, Pennsylvania, 1965.
2. Interim Specifications for Highway Bridges, AASHO Committee on Bridges and Structures, 1966-67.
3. Standard Specifications for Highway Bridges, adopted by the American Association of State Highway Officials, 1965.
4. Dallam, L. N., " Pushout Tests with High-Strength Bolt Shear Connectors ", Missouri Cooperative Highway Research Program Report 68-7, Engineering Experiment Station, University of Missouri - Columbia, 1968.
5. Dallam, L. N., and Harpster, J. L., " Composite Beam Tests with High-Strength Bolt Shear Connectors ", Missouri Cooperative Highway Research Program Report 68-3, Engineering Experiment Station, University of Missouri - Columbia, 1968.
6. Dallam, L. N., and Gaudini, P. B., " Static Behavior of Continuous-Composite-Bolted Beams ", Missouri Cooperative Highway Research Program Report 69-3, Engineering Experiment Station, University of Missouri - Columbia, 1969.
7. Slutter, R. G., and Fisher, J. W., " Fatigue Strength of Shear Connectors ", Steel Research for Construction, American Iron and Steel Institute Bulletin #5, October, 1967.
8. Manual of Steel Construction, American Institute of Steel Construction, Inc., 1967.
9. " Specifications for Structural Joints Using ASTM A325 or A490 Bolts ", American Institute of Steel Construction, Research Council on Riveted and Bolted Structural Joints of the Engineering Foundation, New York, 1964.
10. The AASHO Road Test Report 2, Materials and Construction, HRB Special Report 61B, Appendix E.
11. Proctor, Melvin H., " Analytical and Experimental Study of Lightweight Concrete-Steel Composite Beams ", M. S. Thesis, Department of Civil Engineering, University of Missouri - Columbia, 1963.

12. Viest, I. M., Fountain, R. S., and Singleton, R. C., Composite Construction in Steel and Concrete for Bridges and Buildings, McGraw-Hill Book Company, Inc., New York, 1958.
13. Winter, George, Design of Concrete Structures, McGraw-Hill Book Company, Inc., New York, 1964.
14. Teraszkiewicz, J. S., Static and Fatigue Behaviour of Simply Supported and Continuous Composite Beams of Steel and Concrete, Engineering Structures Laboratories, Civil Engineering Department, Imperial College, London, September, 1967.
15. Michales, J., and Wilson, E. N., Structural Mechanics and Analysis, The Macmillan Company, New York, 1965.

MoDOT Library



RD0016351